Theory of electron energy loss in a random system of spheres

R. G. Barrera

Instituto de Física, Universidad Nacional Autónoma de Mexico, Apartado Postal 20-364, 01000 México, Distrito Federal, México

R. Fuchs

Ames Laboratory and Department of Physics and Astronomy, Iowa State University, Ames, Iowa 50011

We derive an expression for the inverse longitudinal dielectric function $\varepsilon^{-1}(k,\omega)$ of a random system of identical spherical particles with dielectric function $\varepsilon_1(\omega)$ in a host with dielectric function $\varepsilon_2(\omega)$. A spectral representation allows us to separate geometrical and material effects by writing $\varepsilon^{-1}(k,\omega)$ in terms of a spectral function, which depends only on the wave vector k and the geometry of the system. Multipoles of arbitrary order are included. Using a mean-field theory and introducing the two-particle correlation function, we carry out a configuration average and find a simple result for the spectral function. From the loss function $\mathrm{Im}[-\varepsilon^{-1}(k,\omega)]$ we calculate the energy loss probability per unit path length for fast electrons passing through a system of colloidal aluminum particles.

I. INTRODUCTION

Scanning transmission electron microscopy, together with electron-energy-loss measurements, have been used to study systems with various geometries, such as interfaces and small particles.[1-4] The measured electron-energy-loss spectra depend on both material properties and on the geometrical shapes of the particles or interfaces. Energy-loss spectra have been calculated, using classical dielectric theory, for electrons moving on a definite trajectory past surfaces and particles of various shapes.[5-8] More complicated geometries, such as coated spheres,[9] spheroids,[10] interpenetrating spheres,[11] and spheres embedded in planar surfaces,[12] have also been studied. In the above theories, the energy-loss calculation is based on finding the force on the electron due to the induced electric field at the electron's position, as it moves on its classical trajectory. An alternative approach, which leads to equivalent results for an electron moving past a surface, is to find both the electric and magnetic fields outside the surface, allowing the energy-loss rate to be calculated by integrating the Poynting vector into the surface.[13] This theory has the advantage that if the medium below the surface is inhomogeneous but ordered, a transfer-matrix method[14] can be used to find the reflectance amplitude, which is needed to determine the Poynting vector. However, it appears difficult to use this theory to calculate the energy loss of electrons passing through a disordered inhomogeneous system like the one we will be dealing with here. Moreover, the bulk losses due to electrons passing through the particles are not inherently included in the theory.

The theoretical treatments mentioned above are not well suited for analyzing experiments in which the fast incident electrons do not pass at a well-defined distance from a given particle or interface in the inhomogeneous system. In an experiment of this type, Howie and Walsh[15] measured the energy-loss spectra for electrons incident on colloidal Al particles randomly dispersed in an AlF$_3$ matrix. The electrons passed at random distances from the Al particles, as well as through the interiors of the particles. Loss peaks associated with both surface and bulk plasmon excitations of the particles were observed. Effective-medium theories, commonly used for analyzing optical spectra, were only partially successful in explaining the data. Instead, it was found that a simple model, based on classical electron trajectories which can pass both inside and outside the particles, gave a better explanation of the data.[15] The model included only dipolar surface plasmon excitations, and did not take account of the geometrical arrangement of the spheres. Fujimoto and Komaki[16] constructed a theory of electron energy loss for an electron passing a *single* metallic sphere with a given impact parameter r_0, for r_0 both less than and greater than the sphere radius. The electrons in the sphere were described by a hydrodynamic model, and an average over r_0 was taken. They found energy-loss peaks associated with both multipolar surface plasmon and bulk plasmon excitations.

Although the problem of electron energy loss by a single spherical particle has been solved, this is not true for a random system of many spherical particles. The main difficulty lies in taking account of the interaction among the particles and in performing an adequate average over particle positions. In this paper we consider the energy loss of an electron beam passing through a system of spherical particles of equal radii a, located at random in a host material. The sphere and the host materials are described by local, frequency-dependent dielectric functions. The interaction between the particles is included by keeping multipoles of arbitrary order. The electron-energy-loss spectrum for such a system is calculated from the effective inverse longitudinal dielectric response $\varepsilon^{-1}(k,\omega)$, where the term *effective* arises because $\varepsilon^{-1}(k,\omega)$ is the result of averaging over particle positions.

The method of calculation is conceptually simple, as we shall find in Sec. II. An external potential $V^{\mathrm{ext}}(k,\omega)$ is applied to the system, and the total potential

$V(k,\omega) = V^{\text{ext}}(k,\omega) + V^{\text{ind}}(k,\omega)$ is determined. After taking a configuration average over sphere positions, giving an averaged total potential $\langle V(k,\omega) \rangle$, we find the effective inverse longitudinal dielectric function by taking the ratio $\varepsilon^{-1}(k,\omega) = \langle V(k,\omega) \rangle / V^{\text{ext}}(k,\omega)$. The external potential induces multipoles of all orders on the spheres, and the interaction of the multipolar excitations on different spheres is included in the theory. The theory does not include the effect of transverse fields, an approximation that is valid if the radii of the spheres are small enough for retardation effects to be negligible.

We have found it advantageous to write $\varepsilon^{-1}(k,\omega)$ in the form of a spectral representation in which all geometrical effects are included in a spectral function $g(n)$. This function contains information about the strengths and positions of the bulk and surface modes of the system of spheres, but is independent of the dielectric functions of the two media. By surface modes we mean those excitations in which the induced charge lies at the interface between the spheres and the host. Sum rules related to the total strength and centroid of the excitation spectra are also derived. Then, using a mean-field theory, we carry out the configuration average in terms of the two-particle distribution function. The spectral function breaks into discrete Dirac δ functions associated with coupled multipolar surface modes, and we find a simple result for the strengths and positions of these modes.

In Sec. III we apply this mean-field theory for $\varepsilon^{-1}(k,\omega)$ to calculate the electron-energy-loss probability for some specific systems and a summary of the paper appears in Sec. IV. Most of the details of the derivations are presented in the Appendices.

II. INVERSE LONGITUDINAL DIELECTRIC FUNCTION

A. Electron energy loss in an inhomogeneous system

Since the standard derivations of the relation between the inelastic-scattering cross section, the dynamic structure factor, and the longitudinal dielectric function apply to homogeneous systems, we begin this section with a brief discussion of how our inhomogeneous system can be treated. One uses the Born approximation to treat inelastic scattering of a fast charged particle (the incident electron) by an electronic system which may be inhomogeneous. If the energy loss of the incident electron is $E_I - E_F = E = \hbar\omega$ and the momentum transfer is $\mathbf{K}_I - \mathbf{K}_F = \mathbf{k}$, then the probability per unit time of scattering an electron with energy loss in the range $(E, E + dE)$ and final wave vector $\mathbf{K}_F$ in the solid angle $d\Omega$ is[17,18]

$$\frac{dP(E,\Omega)}{dt} = \frac{1}{(2\pi\hbar^2)^2} m K_F |V_k|^2 S(\mathbf{k},\omega) dE \, d\Omega \ , \quad (1)$$

where $V_k = 4\pi e^2/k^2$ and

$$S(\mathbf{k},\omega) = \sum_n |(\rho_{\mathbf{k}})_{n0}|^2 \delta(\omega_{n0} - \omega) \quad (2)$$

is the dynamic structure factor. Here $\rho_{\mathbf{k}} = \sum_j e^{-i\mathbf{k}\cdot\mathbf{r}_j}$ is the density operator, $(\rho_{\mathbf{k}})_{n0}$ is the matrix element of the density operator between exact ground states and excited

states of the electronic system, and ω_{n0} is the excitation frequency. The above equations are written for a system at zero temperature, but only slight modifications are required for the theory to be applied to nonzero temperatures.

Next, we discuss how $S(\mathbf{k},\omega)$ is related to the dielectric function. In an inhomogeneous electronic system the Fourier transform of the inverse dielectric function depends on two wave vectors $\mathbf{k}'$, $\mathbf{k}''$, since a single spatial Fourier component $\rho^{\text{ext}}(\mathbf{k}'',\omega)$ of an external charge density with wave vector $\mathbf{k}''$ can induce a total charge density $\rho^{\text{tot}}(\mathbf{k}',\omega)$ with many Fourier components with wave vectors $\mathbf{k}'$; that is,

$$\rho^{\text{tot}}(\mathbf{k}',\omega) = \sum_{\mathbf{k}''} \varepsilon^{-1}(\mathbf{k}',\mathbf{k}'',\omega) \rho^{\text{ext}}(\mathbf{k}'',\omega) \ . \quad (3)$$

If linear-response theory is applied to this electronic system, turning on a small external charge density adiabatically and calculating the induced and total charge density, one finds a formal expression for the inverse dielectric function:

$$\varepsilon^{-1}(\mathbf{k}',\mathbf{k}'',\omega) = \delta_{\mathbf{k}'\mathbf{k}''} - \frac{4\pi e^2}{\hbar k''^2} \sum_n \left[\frac{(\rho_{\mathbf{k}'})_{n0}(\rho_{\mathbf{k}''})_{n0}^*}{\omega + \omega_{n0} + is} - \frac{(\rho_{\mathbf{k}'})_{n0}^*(\rho_{\mathbf{k}''})_{n0}}{\omega - \omega_{n0} + is} \right] , \quad (4)$$

where s is a small positive quantity.[18] Taking the imaginary part of Eq. (4), we have, for $\mathbf{k}' = \mathbf{k}'' = \mathbf{k}$ and positive ω,

$$\text{Im}\,\varepsilon^{-1}(\mathbf{k},\mathbf{k},\omega) = -\frac{4\pi^2 e^2}{\hbar k^2} \sum_n |(\rho_{\mathbf{k}})_{n0}|^2 \delta(\omega - \omega_{n0})$$

$$= -\frac{4\pi^2 e^2}{\hbar k^2} S(\mathbf{k},\omega) \ . \quad (5)$$

In the above equations $S(\mathbf{k},\omega)$ can depend on the direction of the wave vector, since the theory applies to a general inhomogeneous system. We assume that the system, although inhomogeneous on a microscopic, or more properly, on a mesoscopic scale, is homogeneous and isotropic on a macroscopic scale. Therefore, by taking a suitable ensemble average over the positions of the particles, the system will become isotropic, so the averaged k-dependent quantities in the equations will depend only on the magnitude of the wave vector. Denoting the ensemble average by $\langle \ \rangle$, the isotropic, or effective dynamic structure factor is defined by $S(k,\omega) = \langle S(\mathbf{k},\omega) \rangle$. From Eq. (5) we have

$$S(k,\omega) = -\frac{\hbar k^2}{4\pi^2 e^2} \text{Im}\,\varepsilon^{-1}(k,\omega) \ , \quad (6)$$

where the effective inverse longitudinal dielectric function $\varepsilon^{-1}(k,\omega)$ of the macroscopically isotropic inhomogeneous system is given by

$$\varepsilon^{-1}(k,\omega) = \langle \varepsilon^{-1}(\mathbf{k},\mathbf{k},\omega) \rangle \quad (7)$$

$$= \langle \rho^{\text{tot}}(\mathbf{k},\omega) \rangle / \rho^{\text{ext}}(\mathbf{k},\omega) \ . \quad (8)$$

The last equation is found by taking a single wave vector

$\rho^{\text{ext}}(\mathbf{k}'',\omega) = \rho^{\text{ext}}(\mathbf{k},\omega)\delta_{\mathbf{k}\mathbf{k}''}$ on the right-hand side of Eq. (3), choosing a single Fourier component $\mathbf{k}' = \mathbf{k}$, the same as that of the external charge density, from the total charge density on the left-hand side of Eq. (3), and taking an ensemble average. Now, since $4\pi\rho^{\text{ext}}(\mathbf{k},\omega) = k^2 V^{\text{ext}}(\mathbf{k},\omega)$ and

$$4\pi\rho^{\text{tot}}(\mathbf{k},\omega) = k^2 V(\mathbf{k},\omega)$$
$$= k^2[V^{\text{ext}}(\mathbf{k},\omega) + V^{\text{ind}}(\mathbf{k},\omega)] ,$$

Eq. (8) can be written as

$$\varepsilon^{-1}(k,\omega) = 1 + \langle V^{\text{ind}}(\mathbf{k},\omega)\rangle / V^{\text{ext}}(\mathbf{k},\omega) , \quad (9)$$

which is the form we shall use to perform the actual calculation of $\varepsilon^{-1}(k,\omega)$. Recall that we are assuming, from the beginning, that both the sphere and the host materials have a local (k-independent) dielectric response; therefore, the k dependence or nonlocality of $\varepsilon^{-1}(k,\omega)$ arises from the finite sphere size and the interaction between spheres.

B. Basic formalism for finding $\varepsilon^{-1}(k,\omega)$

Our system consists of N spheres of radius a located at random positions $\mathbf{r}_i$ in a box of volume v. The spheres and the host are made of materials with local, isotropic, dielectric functions $\varepsilon_1(\omega)$ and $\varepsilon_2(\omega)$, respectively. In order to simplify the notation we replace the dielectric function of the spheres, $\varepsilon_1(\omega)$, by $\varepsilon(\omega)$ and that of the host, $\varepsilon_2(\omega)$, by 1. At the end of the calculation we will restore the original materials by replacing $\varepsilon(\omega)$ by the ratio $\varepsilon_1(\omega)/\varepsilon_2(\omega)$, and $\varepsilon^{-1}(k,\omega)$ by $\varepsilon^{-1}(k,\omega)\varepsilon_2(\omega)$.

We start with an external potential with a single Fourier component with wave vector $\mathbf{k}$. It is convenient to take $\mathbf{k}$ in the z direction, so the external potential can be written

$$V^{\text{ext}}(\mathbf{r},t) = V^{\text{ext}}(\mathbf{r})e^{-i\omega t} = V_0 e^{ikz}e^{-i\omega t} . \quad (10)$$

From Eqs. (10) and (A11), the kth Fourier component of the external potential is $V^{\text{ext}}(k,\omega) = V_0$. We will further simplify the arguments in the induced potential by dropping the index ω, so that $V^{\text{ind}}(k,\omega)$ is written simply as $V^{\text{ind}}(k)$.

The external potential induces charges on the spheres, and there are multipoles associated with the distribution of these charges on each sphere, so one has a system of coupled multipoles, driven by the external potential. After having solved for the induced multipoles, we can find the induced potential $V^{\text{ind}}(\mathbf{r})$ produced by all the induced charges on the spheres. The quantity of interest, $V^{\text{ind}}(k)$, is the kth Fourier component of $V^{\text{ind}}(\mathbf{r})$.

We now proceed to carry out the calculation described in the preceding paragraph. The multipole q_{lmi} on sphere i can be written as the sum of two terms,

$$q_{lmi} = q_{lmi}^0 + q_{lmi}^1 , \quad (11)$$

where q_{lmi}^0 is the multipole produced by the external potential acting on sphere i, and q_{lmi}^1 is produced by the induced potential arising from all spheres j different from i, acting on sphere i. Since the external potential has an e^{ikz} dependence, it induces only $m = 0$ multipoles on the

spheres, so $q_{lmi}^0 = q_{l0i}^0 \equiv q_{li}^0$. This induced multipole q_{li}^0 must be proportional to the external potential V_0, and it contains the phase factor e^{ikz_i}, so it can be written in the form

$$q_{li}^0 = F_l V_0 e^{ikz_i} . \quad (12)$$

An expression for F_l is derived in Appendix B.

The induced multiple q_{lmi}^1 on sphere i is proportional to the induced potential acting on the same sphere, and can be written

$$q_{lmi}^1 = -\frac{2l+1}{4\pi}\alpha_l V_{lmi}^1 . \quad (13)$$

Here α_l is the l polarizability of a sphere and V_{lmi}^1 is the coefficient in the spherical harmonic expansion, about the center of sphere i, of the induced potential arising from spheres j different from i:

$$V^{1,\text{ind}}(\mathbf{r}') = \sum_{lm} V_{lmi}^1 (r')^l Y_{lm}(\theta',\varphi') , \quad (14)$$

where $\mathbf{r}' = (r',\theta',\varphi') = \mathbf{r} - \mathbf{r}_i$. The coefficient V_{lmi}^1 is determined by the induced multipoles $q_{l'm'j}$ on spheres j different from i by the equations of the form

$$V_{lmi}^1 = \sum_{l'm'j} B_{lmi}^{l'm'j} q_{l'm'j} . \quad (15)$$

Expressions for the coefficients $B_{lmi}^{l'm'j}$ are given in Appendix D. Combining Eqs. (11), (13), and (15), we get a set of coupled equations for the multipoles on all spheres:

$$q_{lmi} = q_{li}^0 \delta_{m0} - \frac{2l+1}{4\pi}\alpha_l \sum_{l'm'j} B_{lmi}^{l'm'j} q_{l'm'j} . \quad (16)$$

Equation (16) can be solved using a spectral-representation method, as will be described in detail in Appendix D. The key step in the solution is to write Eq. (16) in the form

$$\sum_{l'm'j} \left[\left[\frac{1}{\varepsilon-1} + n_l^0 \right] \delta_{ll'}\delta_{mm'}\delta_{ij} + h_{lmi}^{l'm'j}(k) \right] y_{l'm'j}$$
$$= -\frac{(-i)^l}{4\pi}\sqrt{la^{2l+1}} R_l V_0 \delta_{m0} , \quad (17)$$

where

$$y_{lmi} = q_{lmi}\frac{(-i)^l}{\sqrt{la^{2l+1}}}e^{-ikz_i} . \quad (18)$$

Here $n_l^0 = 1/(2l+1)$ are depolarization factors for the surface resonances of an isolated sphere, and $h_{lmi}^{l'm'j}(k)$ is a real Hermitian matrix that is independent of the properties of the material. These properties appear only in the term $1/(\varepsilon-1)$ in the diagonal element on the left-hand side of Eq. (17). Expressions for $h_{lmi}^{l'm'j}(k)$ and R_l are given in Appendix D. The structure of this equation is what allows us to find a solution in the form of a spectral representation, in which the depolarization factors for the surface resonances of the coupled system of spheres are the eigenvalues of the matrix $H_{lmi}^{l'm'j}(k)$ $= n_l^0 \delta_{ll'}\delta_{mm'}\delta_{ij} + h_{lmi}^{l'm'j}(k).$

Equation (17) is valid for an arbitrarily large number of spheres at random locations; it can be solved formally to give sum rules, as we shall show in Appendix F, but this formal exact solution is not useful for the actual calculation of $\varepsilon^{-1}(k,\omega)$. Here we present an approximate solution of Eq. (17) by using a mean-field theory. This means, that for all spheres, we neglect the fluctuations of the multipoles about their average values, and take the multipole on each sphere to be equal to its corresponding average. Therefore, all multipoles are "aligned" in the z direction; that is, only the $m=0$ multipoles appear. This allows us to write the multipole variables as $y_{l'm'j}=\langle y_{l'}\rangle\delta_{m'0}$, which no longer depend on the sphere index j. The ensemble average of Eq. (17), over a large number of random sphere configurations, becomes

$$\sum_{l'}\left[\left[\frac{1}{\varepsilon-1}+n_l^0\right]\delta_{ll'}+\left\langle\sum_j h_{li}^{l'j}(k)\right\rangle\right]\langle y_{l'}\rangle$$
$$=-\frac{(-i)^l}{4\pi}\sqrt{la^{2l+1}}R_lV_0 \ . \quad (19)$$

Here $\langle\sum_j h_{li}^{l'j}(k)\rangle$ is the ensemble average of the multipolar interaction between spheres, which depends on the two-particle distribution function, as shown in detail in Appendix D.

Equation (19) can be solved immediately for $\langle y_{l'}\rangle$, and then the corresponding average multiple $\langle q_{li}\rangle$ is found by using Eq. (18). The result has the following structure:

$$\langle q_{li}\rangle=\sum_{sl'}\frac{D_{ll'}(s)}{(\varepsilon-1)^{-1}+n_s}R_{l'}V_0e^{ikz_i} \ , \quad (20)$$

where n_s are the depolarization factors of the surface modes of the coupled system of spheres, and are given by the eigenvalues of a matrix $H_{ll'}=n_l^0\delta_{ll'}+\langle\sum_j h_{li}^{l'j}(k)\rangle$. The coefficients $D_{ll'}(s)$ are related to the eigenvectors of $H_{ll'}$, as is also shown in Appendix D. Note that n_s and $D_{ll'}(s)$ are independent of the dielectric function $\varepsilon(\omega)$, but depend only on geometrical factors: the wave vector k, the sphere radius a, the volume fraction of spheres, and their two-particle distribution function.

The final step is to find $V^{ind}(k)$, the kth Fourier component of the induced potential. We express $V^{ind}(k)$ as a sum of contributions from the individual spheres:

$$V^{ind}(k)=\sum_i V_i^{ind}(k) \ . \quad (21)$$

The contribution $V_i^{ind}(k)$ from sphere i can be written as a sum of two parts:

$$V_i^{ind}(k)=V_i^{ind,0}(k)+V_i^{ind,1}(k) \ , \quad (22)$$

which are defined similarly to Eq. (11). The external potential, with a single Fourier component k, induces charges on sphere i with multipole moments q_{lmi}^0. These induced charges produce an induced potential $V_i^{ind,0}(\mathbf{r})$, which has the kth Fourier component $V_i^{ind,0}(k)$. The potential from spheres other than sphere i also acts on sphere i, inducing charges that have multipole moments q_{lmi}^1. These induced charges produce an induced potential $V_i^{ind,1}(\mathbf{r})$, with a kth Fourier component $V_i^{ind,1}(k)$.

Therefore, $V_i^{ind,0}(k)$ must be proportional to the external potential V_0, and we can write

$$V_i^{ind,0}(k)=\sum_{l=0}^{\infty}M_lV_0 \ , \quad (23)$$

where the coefficients M_l are given in Appendix A. Similarly, $V_i^{ind,1}(k)$ is proportional to the induced multipoles q_{lmi}^1:

$$V_i^{ind,1}(k)=\sum_{l=1}^{\infty}Z_lq_{li}^1e^{-ikz_i}$$
$$=\sum_{l=1}^{\infty}Z_l(q_{li}-q_{li}^0)e^{-ikz_i} \ , \quad (24)$$

where we have dropped the m index because only $m=0$ multipoles contribute. The phase factor e^{-ikz_i} is included to cancel the factor e^{ikz_i} that occurs in q_{li}^1, so no phase factor appears in the expressions for the coefficients Z_l, as can be seen in Appendix C.

Using Eqs. (23), (24), and (12), we can rewrite Eq. (22),

$$V_i^{ind}(k)=\sum_{l=0}^{\infty}[(M_l-Z_lF_l)V_0+Z_lq_{li}e^{-ikz_i}] \ . \quad (25)$$

We take the ensemble average of Eq. (25) and use Eq. (20) for $\langle q_{li}\rangle$. The sum over i in Eq. (21) gives a factor N, so we find

$$\langle V^{ind}(k)\rangle=N\left[\sum_{l=0}^{\infty}(M_l-Z_lF_l)+\sum_{sll'}\frac{Z_lD_{ll'}(s)R_{l'}}{(\varepsilon-1)^{-1}+n_s}\right]V_0 \ . \quad (26)$$

The inverse dielectric function is then given by $\varepsilon^{-1}(k,\omega)=1+\langle V^{ind}(k)\rangle/V_0$.

C. Spectral representation for $\varepsilon^{-1}(k,\omega)$

The spectral representation of the effective dielectric response of a composite, in the local limit $(k\rightarrow 0)$, was first introduced by Bergman[19] and Milton.[20] They showed that the local effective dielectric function of any two-component material is a function of the ratio of the dielectric functions of its components, and also, that this function can be always written as a series of simple poles and residues which depend only on the microgeometry of the composite material and not on the dielectric functions of the components. However, if the microgeometry is random, in the limit of infinite volume, the poles merge into a branch cut and the residues become a continuous function, called the spectral function.

Fuchs and Claro,[21] and later on Hinsen and Felderhof,[22] developed two different procedures for the calculation, in the long-wavelength limit, of these poles and residues for a finite system of identical spheres embedded in an otherwise homogeneous host. Here we extend the formalism of Fuchs and Claro[21] to the effective inverse longitudinal dielectric response, but now with a finite wave vector.

For doing this, the quantities in Eq. (26) can be simplified and combined, as discussed in Appendix E, to

provide an expression of $\varepsilon^{-1}(k,\omega)$ as a series of simple poles and residues. We obtain

$$\varepsilon^{-1}(k,\omega)=(\varepsilon_2)^{-1}\left[1+f\left[\frac{C_b}{u-1}+\sum_s\frac{C_s}{u-n_s}\right]\right], \quad (27)$$

where f is the volume fraction of the spherical particles and u is a spectral variable, defined as

$$u=-(\varepsilon_1/\varepsilon_2-1)^{-1}. \quad (28)$$

Here we have replaced $\varepsilon^{-1}(k,\omega)$ by $\varepsilon^{-1}(k,\omega)\varepsilon_2$ and ε by $\varepsilon_1/\varepsilon_2$, a complex function of the frequency, in order to return to the original materials, where the spheres and the host have dielectric functions ε_1 and ε_2, respectively.

Equation (27) is one of the main results of our paper. It is a spectral representation of $\varepsilon^{-1}(k,\omega)$, in which the residue C_b is the strength of the bulk longitudinal mode and the residues C_s are surface mode strengths. The frequencies of the modes are determined by the poles of each term, that is, by the vanishing of the corresponding denominators. For the bulk mode the depolarization factor is $n_b=1$, and so the denominator vanishes if $u=n_b=1$, or $\varepsilon_1(\omega)/\varepsilon_2(\omega)=0$. The surface modes, labeled by the index s, have depolarization factors n_s and their frequencies are determined by $u=n_s$ or $\varepsilon_1(\omega)/\varepsilon_2(\omega)=1-1/n_s$.

The bulk mode strength is

$$C_b=1-3\sum_{l=1}^{\infty}l(2l+1)[j_l(\rho)/\rho]^2. \quad (29)$$

Notice that the strength of the bulk mode now differs from 1, and that the difference does not depend on the geometrical arrangement of spheres, but only depends on the sphere radius through $\rho=ka$. This means that the depression of the strength of the bulk mode comes from the finite size of the spheres. This depression in strength is known in the literature as the *Begrenzung* effect.[23]

On the other hand, the properties of the surface modes (n_s and C_s) depend on interactions between the spheres and, within the mean-field theory, are determined by the eigenvalues and eigenvectors of a real symmetric matrix $H_{ll'}$, which is a functional of only the two-particle distribution function $\rho^{(2)}(r)$. Explicit expressions for $H_{ll'}$, in terms of $\rho^{(2)}(r)$, are given in Eqs. (D13)–(D16) of Appendix D. For simplicity, we consider here only the excluded-volume correlation among pairs of particles; that is, we take $\rho^{(2)}(r)=n\theta(r-r_0)$, where $n=N/v$ is the density of spheres, $\theta(x)$ is the step function, and $r_0=2a$ is the exclusion radius. The result is

$$H_{ll'}=\frac{l}{2l+1}\delta_{ll'}$$
$$+3f\sqrt{ll'/(2l+1)(2l'+1)}\frac{(l+l')!}{l!(l')!}\left[\frac{a}{r_0}\right]^{l+l'-2}$$
$$\times\frac{j_{l+l'-1}(kr_0)}{kr_0}, \quad (30)$$

where $j_\nu(x)$ is the spherical Bessel function of order ν.

The depolarization factors of the surface modes are the

eigenvalues of $H_{ll'}$, and their strengths are related to its eigenvectors through the unitary matrix U_{sl} which diagonalizes $H_{ll'}$. That is,

$$\sum_{ll'}U_{sl}^{-1}H_{ll'}U_{l's'}=n_s\delta_{ss'}. \quad (31)$$

The strengths of the surface modes are given by

$$C_s=3\sum_{ll'}\sqrt{ll'(2l+1)(2l'+1)}\rho^{-2}j_l(\rho)j_{l'}(\rho)U_{ls}U_{l's}, \quad (32)$$

where $\rho=ka$.

Therefore, we obtain an expression for the *inverse* longitudinal dielectric function $\varepsilon^{-1}(k,\omega)$ with the same structure and the *same* spectral variable, as the one proposed originally by Bergman[19] and Milton[20] for the local effective dielectric function $\varepsilon_{\mathrm{eff}}(\omega)$. The main difference is that values of the poles and residues are now k dependent.

It can be easily shown (see Appendix F) that the strengths of all modes add up to 1:

$$C_b+\sum_s C_s=1, \quad (33)$$

and that $\sum_s C_s n_s$, the first moment of the surface mode spectrum, is given by

$$\sum_s C_s n_s=\sum_{ll'}3\sqrt{ll'(2l+1)(2l'+1)}\rho^{-2}j_l(\rho)j_{l'}(\rho)H_{ll'}. \quad (34)$$

It is also shown in Appendix F, that both of these sums rules are valid not only within the mean-field theory, but that they are valid in general. This means that they also apply to an exact theory.

Now we consider the $k\rightarrow0$ (local) limit of $\varepsilon^{-1}(k,\omega)$ within the mean-field theory. From Eq. (30) we find $H_{11}=(1+2f)/3$, $H_{ll}=l/(2l+1)$ if $l>2$, and $H_{ll'}=0$ for $l\neq l'$. Modes with different l values are uncoupled since off-diagonal elements of $H_{ll'}$ vanish, so the surface modes can be labeled by the multipole index l. Furthermore, the bulk mode strength is $C_b=0$, the dipole ($l=1$) surface mode has strength $C_l=1$, and the higher-multipole modes have zero strengths: $C_l=0$ for $l\geq2$. Equation (27) becomes

$$\varepsilon^{-1}(0,\omega)=(\varepsilon_2)^{-1}[1+f/(u-n_1)], \quad (35)$$

where $n_1=\frac{1}{3}(1+2f)$. Thus at $k=0$, the longitudinal dielectric function reduces to the Maxwell-Garnett (MG) dielectric function $\varepsilon_{\mathrm{MG}}(\omega)$, which can be considered as the $k=0$ limit of the transverse dielectric function for a system of spherical particles within the mean-field theory.[24] That is, Eq. (35) can be rewritten,

$$\varepsilon(0,\omega)=\varepsilon_2[1-f/(u-n_{\mathrm{MG}})]\equiv\varepsilon_{\mathrm{MG}}(\omega), \quad (36)$$

where $n_{\mathrm{MG}}=\frac{1}{3}(1-f)$. For this reason our theory can be considered a generalization of the MG theory to finite wavelength and to all multipolar orders. It also explains why a straightforward application of an effective-medium

theory like MG, which is successful in the optical range ($k \to 0$), fails to give reasonable answers when applied to electron-energy-loss experiments, where the k dependence of the external field plays a prominent role.

An alternative way of writing the spectral representation of $\varepsilon^{-1}(k,\omega)$ is[25]

$$\varepsilon^{-1}(k,\omega) = \frac{1-f}{\varepsilon_2} \left[1 - \frac{f}{1-f} \sum_s \left[\frac{1}{n_s} - 1 \right] C_s \right]$$
$$+ \frac{f}{\varepsilon_1} \left[1 - \sum_s C_s \right] + f \sum_s \frac{C_s/n_s}{n_s \varepsilon_1 + (1-n_s)\varepsilon_2} ,$$

(37)

where we have eliminated the spectral variable u in favor of the dielectric functions ε_1 and ε_2, and have replaced C_b by $1 - \sum_s C_s$, using the sum rule in Eq. (33). In this expression, the first term has a pole at $\varepsilon_2 = 0$, and thus is interpreted as the contribution of the bulk mode of the host, with a weight proportional to the filling fraction of the host: $1-f$, times a factor less than 1, which represents the *Begrenzung* effect in the host. The second term in Eq. (37) has a pole at $\varepsilon_1 = 0$, so it corresponds to the contribution of the bulk mode of the spheres, with a weight proportional to the filling fraction of the spheres (f), times $1 - \sum_s C_s$, which represents the Begrenzung effect in the spheres, as pointed out before. Finally, the third term in Eq. (37) corresponds to the contribution of the surface modes of the system. The location of the surface modes here is the same as in Eq. (33), since the zeros of the denominators here are the same as the zeros of $u - n_s$. This form of the spectral representation of $\varepsilon^{-1}(k,\omega)$ might be useful to people working in electron-energy-loss spectroscopy, who often interpret experiments in terms of excitation functions for each material. Notice, however, that our theory is, from the start, non-symmetric with respect to the role played by materials 1 and 2. For any filling fraction f, material 1 consists of identical inclusions of spherical shape, and thus is disconnected, while material 2 is always connected and plays the role of the host. Therefore, while the shape of the inclusions is independent of f, the shape of the host depends on f. For this reason, the *Begrenzung* effect is independent of f for the spheres but is f dependent for the host.

D. Numerical results

As mentioned before, one of the distinguishing merits of the spectral representation of $\varepsilon^{-1}(k,\omega)$, as given by Eqs. (27)–(32), is that both the mode strengths and the mode positions are independent of the materials. In this section we present numerical calculations of their dependence on the filling fraction f, the wave vector k, and the sphere radius a. Since we are considering only the excluded-volume correlations among pairs of spheres, the dependence on k and a will always appear as the product ka.

In Fig. 1 we show C_b as a function of ka, for different values of L_{max}, which is defined as the maximum value of l taken in the multipolar sum of Eq. (29). This figure
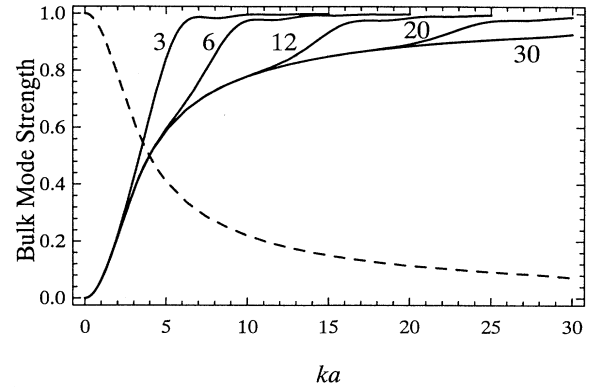

FIG. 1. The solid lines show the bulk mode strength C_b as a function of ka calculated with different values of L_{max}. The numbers which label the different solid lines designate the corresponding value of L_{max} used in the calculation. The dashed line is the total strength of the surface modes, $1 - C_b$.

shows that as the value of ka increases, more terms must be included in the multipolar sum. For example, for $ka = 10$ a value $L_{max} = 12$ is sufficient, whereas for $ka = 20$, $L_{max} = 20$ is required. Also, it can be seen that $C_b = 0$ for $ka = 0$, increases as $(ka)^2$ for small ka, and finally approaches 1 asymptotically for large values of ka. Thus for a fixed value of k and $a \to \infty$, C_b tends to its bulk value: 1. According to the sum rule in Eq. (33), this reduction in the strength of the bulk mode (*Begrenzung* effect) is equal to the sum of the strengths of all the surface modes of the system. In Fig. 1 the total strength of the surface modes is also plotted as a function of ka. It has the value 1 when $ka = 0$, and then decreases as ka increases. For example, when $ka = 10$, the total strength of the surface modes is about 0.22.

We now consider the position and strength of each individual surface mode. When $k > 0$, we have $H_{ll'} \neq 0$ if $l \neq l'$, so different multipoles are coupled, and the surface modes cannot be labeled by the index l. Nevertheless, as can be seen from Eq. (30), the eigenvalues n_s of $H_{ll'}$ in the $k \to 0$ limit are easily determined. For $l = 1$, as pointed out before, $n_1 = (1+2f)/3$, and for $l > 1$, $n_l = l/(2l+1)$, independent of the filling fraction f. Therefore we will denote the different surface modes by taking the label s equal to the corresponding value of l at $k = 0$.

Figure 2(a) shows the mode positions, i.e., the surface mode depolarization factors n_s, as functions of ka, for $f = 0.1$ and $L_{max} = 6$ is the dimensionality of the matrix $H_{ll'}$. The $s = 1$ and $s = 2$ modes, which happen to be degenerate at $k = 0$, split rapidly as ka increases. This accidental degeneracy arises because $n_1 = (1+2f)/3$ is equal to $n_l = l/(2l+1)$, for $f = 0.1$ and $l = 2$. Figure 2(b) shows the mode positions $n_s(ka)$ for $f = 0.5$ and $L_{max} = 6$. At $k = 0$, the dipole mode is shifted to $n_1 = 2/3$; as k increases, this "dipole" mode moves to smaller values of n_1 and then, around $ka = 3$, it flattens out, at values of n_1 of about 0.48. In both cases, $f = 0.1$ and $f = 0.5$, the higher modes ($s > 3$) show a small

dispersion with respect to ka, this dispersion being smaller the higher the mode.

In Figs. 3(a) and 3(b), the mode strengths C_s are plotted as functions of ka, for values of $f = 0.1$ and 0.5, respectively, and $L_{max} = 6$. We also plot the total strength of the six surface modes (dashed line) and also the exact total strength of all surface modes, $\sum_s C_s = 1 - C_b$, using the sum rule given in Eq. (33). These two curves coincide all the way up to $ka \approx 5$, and as mentioned above, are independent of f. This means that up to this value of ka, the first six modes exhaust the sum rule, and one might expect that the contribution of higher modes should not be important. Figure 3(b), with $f = 0.5$, shows that the "dipole" $(s = 1)$ mode is the only mode with a finite strength at $ka = 0$, and that this strength decreases as ka increases. On the other hand, the strengths of all other modes start with zero values at $ka = 0$, increase as ka increases, go through a maximum, and finally decrease asymptotically to zero for large values of ka. This maximum shifts to larger values of ka, the higher the mode index. The behavior of $C_s(ka)$ for $f = 0.1$ is similar, as can be seen in Fig. 3(a). However, it might seem in this figure that the first two modes share strengths equally for

$ka \approx 0$. This is not true, and a closer look at the region of very small values of ka shows that at $ka = 0$, the $s = 1$ and $s = 2$ modes actually start with strengths equal to 1 and 0, respectively. Then, very rapidly, both strengths become approximately equal to 0.5 at about $ka = 0.1$, and as ka continues to increase, they separate slowly and progressively. This behavior is due to the accidental degeneracy of these two modes at $ka = 0$.

We now illustrate the effects of the multipolar coupling and how the l character of the modes is preserved, lost, and eventually transferred to other modes, depending on the strength of the coupling in different regions of ka. We do this by showing in Figs. 4(a) and 4(b) the mode positions $n_s(ka)$ without coupling between different multipoles, for $f = 0.1$ and $f = 0.5$, and then comparing them with the corresponding mode positions in Figs. 2(a) and 2(b). The multipolar coupling is taken away by simply neglecting all the nondiagonal matrix elements in the matrix $H_{ll'}$. One can see, by comparing Figs. 2(a) and 4(a), that for $f = 0.1$ the effect of multipolar coupling is hardly
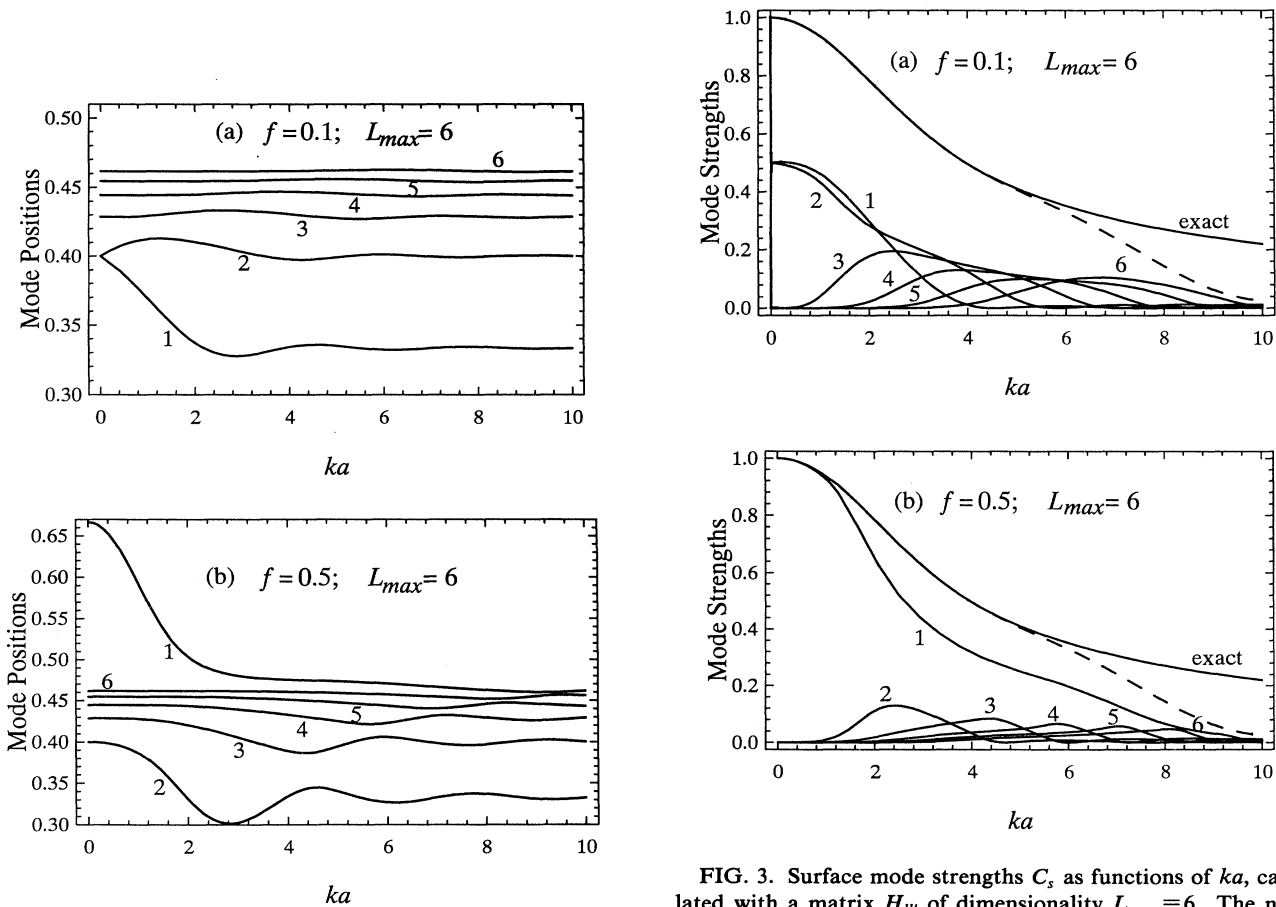

FIG. 2. Surface mode positions n_s as functions of ka, calculated with a matrix $H_{ll'}$ of dimensionality $L_{max} = 6$. The numbers which label the different curves correspond to the surface mode index s. Plot (a) is for $f = 0.1$; plot (b) is for $f = 0.5$.

FIG. 3. Surface mode strengths C_s as functions of ka, calculated with a matrix $H_{ll'}$ of dimensionality $L_{max} = 6$. The numbers which label the different curves correspond to the surface mode index s. Plot (a) is for $f = 0.1$; plot (b) is for $f = 0.5$. The dashed line is the total strength of the six surface modes shown, and the line labeled "exact" is the total strength of all surface modes, $1 - C_b$.

noticeable; thus all the modes preserve, very much, their original ($k=0$) l character. On the other hand, by comparing Figs. 2(b) and 4(b), one can see that for $f=0.5$, the effects of coupling are rather strong, especially for values of $ka \le 4$. That is, the ka region where the uncoupled modes cross is the region where the effect of multipolar coupling is the strongest. As expected, the main effect of multipolar coupling is to "repel" the modes so they actually do not cross. Thus in the region $ka \le 4$, where the "crossing" of modes occurs, the modes lose their original ($k=0$) l character. When $ka \gtrsim 5$, the modes regain their original l character, but now the dipolar character has been transferred to mode $s=2$, while the $l=6$ character has been transferred to mode $s=1$.

For larger values of L_{max} (>6), a corresponding larger number of modes will appear, with values of n_s between 6/13 and 1/2 at $k=0$, the value 1/2 being an accumulation point. These higher modes will be rather flat with respect to ka and will lie very close to each other. We have chosen the rather small value, $L_{max}=6$ (giving six modes), in order to provide the clearest possible illustration of the mode positions as functions of ka. If we had

shown more modes by taking a larger value of L_{max}. Figs. 2–4 would have been very confusing because of the high density of the additional modes and intricate behavior of the modes in the "crossing regions."

The nice thing about the numerical results presented here is that they are independent of the dielectric properties of the materials of the composite; they depend only on f and ka. Nevertheless in order to give a more physical meaning to the depolarization factor presented above, it is useful to think of specific materials. Let us take the sphere material to be a free-electron gas, with $\varepsilon_1 = 1 - (\omega_{p1})^2/\omega^2$, where ω_{p1} is the plasma frequency, and the host to be vacuum, $\varepsilon_2 = 1$. Then the bulk mode condition $u=1$ or $\varepsilon_1 = 0$ corresponds to the condition $\omega_b = \omega_{p1}$, whereas the surface mode condition $u=n_s$ or $\varepsilon_1 = 1 - n_s^{-1}$ corresponds to the frequency $\omega_s = \omega_{p1}\sqrt{n_s}$. Hence, each depolarization factor or mode position is associated with a specific mode frequency, such that depolarization factors in the range between 0 and 1 correspond to surface mode frequencies in the range between zero and the plasma frequency ω_{p1}, and the bulk mode frequency is the plasma frequency.

III. ELECTRON-ENERGY-LOSS PROBABILITY

A. Basic formalism

In this section we apply our result for $\varepsilon^{-1}(k,\omega)$ to the calculation of the energy loss of a beam of fast electrons passing through the composite. Using Eq. (6), which applies to our effectively isotropic inhomogeneous system, we can write Eq. (1),

$$\frac{dP(E,\Omega)}{dt} = \frac{mK_F e^2}{\pi^2 \hbar^3 k^2} \text{Im}[-\varepsilon^{-1}(k,\omega)] dE \, d\Omega \ . \quad (38)$$

If the wave vector $\mathbf{K}_I$ of the initial electron is in the z direction, the scattering wave vector $\mathbf{k}$ can be decomposed into a components parallel and perpendicular to z: $\mathbf{k} = k_z \hat{z} + Q\hat{\rho}$. We assume that the deflection angle is small, and that the loss in energy is small compared to the initial energy. Then $K_I \approx K_F$, the conditions for energy and momentum conservation give $k_z = \omega/v_I$, where $v_I = \hbar K_I / m$ is the initial speed of the electron, and the solid angle element is $d\Omega = 2\pi \sin\theta \, d\theta \approx 2\pi Q \, dQ/(K_I)^2$. Equation (38) can then be rewritten,

$$\frac{dP(E,\Omega)}{dt} = \frac{2e^2}{\pi \hbar^2 v_I} \text{Im}\left[-\varepsilon^{-1}(k,\omega)\right] \frac{Q \, dQ \, dE}{k^2} \ , \quad (39)$$

with $k^2 = Q^2 + (\omega/v_I)^2$.

We want to find the energy-loss probability per unit path length, for all scattering angles, so we divide Eq. (39) by v_I and integrate over Q. Finally, dividing by dE, we get the probability per unit path length, per unit energy, of scattering with energy loss E:
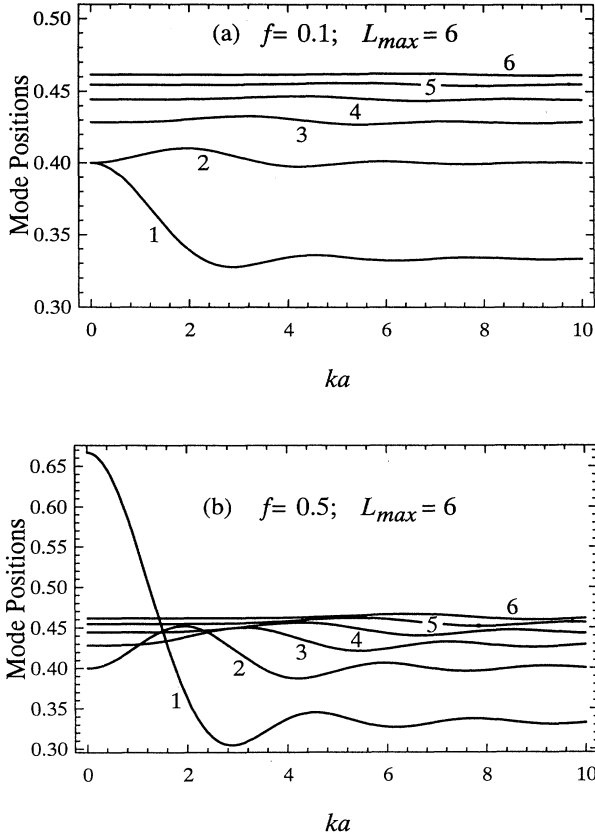

FIG. 4. Surface mode positions n_l as functions of ka, calculated without multipolar coupling and a (diagonal) matrix $H_{ll'}$ of dimensionality $L_{max}=6$. The numbers which label the different curves correspond to the multipolar index l of the surface modes. Plot (a) is for $f=0.1$; plot (b) is for $f=0.5$.

$$F(E) = \frac{d^2 P(E)}{dl \, dE} = (a_0 E_I)^{-1} \Xi(E) \ , \quad (40)$$

where

$$\Xi(E) = \frac{1}{\pi} \int_0^{Q_c} \frac{Q \, dQ}{k^2} \text{Im}\left[-\varepsilon^{-1}(k,\omega)\right] \ . \quad (41)$$

Here a_0 is the Bohr radius, E_I is the incident electron energy, and Q_c is an upper cutoff wave vector that is needed to avoid a logarithmic divergence of the integral. Q_c is determined by $(k_c)^2 = (\omega/v_f)^2 = (Q_c)^2 + (\omega/v_I)^2$, where v_f is the Fermi velocity and k_c is approximately the largest wave vector for which the bulk plasmon is a well-defined excitation. $\Xi(E)$ is the dimensionless energy-loss probability density spectrum which will be calculated and analyzed below.

Within the mean-field theory and taking account only of excluded volume pair correlations, an explicit expression for $\Xi(E)$ is found by substituting Eq. (37) into Eq. (41). The result is

$$\pi\Xi(E) = \left[(1-f)\ln\frac{k_c v_I}{\omega} + f\left(\sum_l B_l - \sum_s K_s\right)\right]\mathrm{Im}\left[\frac{-1}{\varepsilon_2}\right]$$

$$+ f\left[\ln\frac{k_c v_I}{\omega} - \sum_l B_l\right]\mathrm{Im}\left[\frac{-1}{\varepsilon_1}\right] - f\sum_s L_s ,$$

$$(42a)$$

where

$$B_l = 3l(2l+1)\int_{\omega a/v_i}^{k_c a}\frac{j_l^2(x)}{x^3}dx , \qquad (42b)$$

$$K_s = \int_{\omega a/v_I}^{k_c a}\frac{C_s(x)}{n_s(x)}\frac{dx}{x} , \qquad (42c)$$

$$L_s = \int_{\omega a/v_I}^{k_c a}\frac{C_s(x)}{n_s(x)}\mathrm{Im}\left[\frac{1}{n_s(x)\varepsilon_1 + [1-n_s(x)]\varepsilon_2}\right]\frac{dx}{x} . \qquad (42d)$$

Here $C_s(x) \equiv C_s(ka)$ and $n_s(x) \equiv n_s(ka)$ are the strengths and positions of the surface modes as functions of ka, for a given filling fraction f. The contribution to the energy-loss probability due to the excitation of bulk plasmons in medium 1 (2), which is identified by the presence of the bulk loss function $\mathrm{Im}(-1/\varepsilon_1)[\mathrm{Im}(-1/\varepsilon_2)]$, is given by the first (second) term on the right-hand side of Eq. (42a). The third term on the right-hand side of this equation represents the contribution to the energy-loss probability due to the excitation of surface or interfacial modes.

We can take the dilute limit $(f \to 0)$ in Eq. (42) with $\varepsilon_2 = 1$. In this case, the matrix $H_{ll'}$ becomes diagonal and its eigenvalues are $n_l = l/(2l+1)$. Also, since $U_{ls} = \delta_{ls}$, Eq. (32) gives $C_s = 3s(2s+1)[j_s(ka)/ka]^2$, and we can write, to lowest order of f,

$$\lim_{f\to 0}\Xi(E) = f\left\{\frac{1}{\pi}\left[\ln\frac{k_c v_I}{\omega} - \sum_{l=1}^{\infty}B_l\right]\mathrm{Im}\left[\frac{-1}{\varepsilon_1}\right]\right.$$

$$\left. + \sum_{l=1}^{\infty}(2l+1)B_l\frac{1}{\pi}\mathrm{Im}\left[\frac{\varepsilon_1+1}{l\varepsilon_1+l+1}\right]\right\} . \qquad (43)$$

Since the right-hand side of Eq. (43) is directly proportional to f, the term in curly brackets represents the con-

tribution to the energy-loss probability from a single, isolated sphere in vacuum. It has two terms; the first term is due to the excitation of bulk plasmons in the sphere, and the second term is due to the excitation of the surface modes. This expression agrees exactly with the one ob-
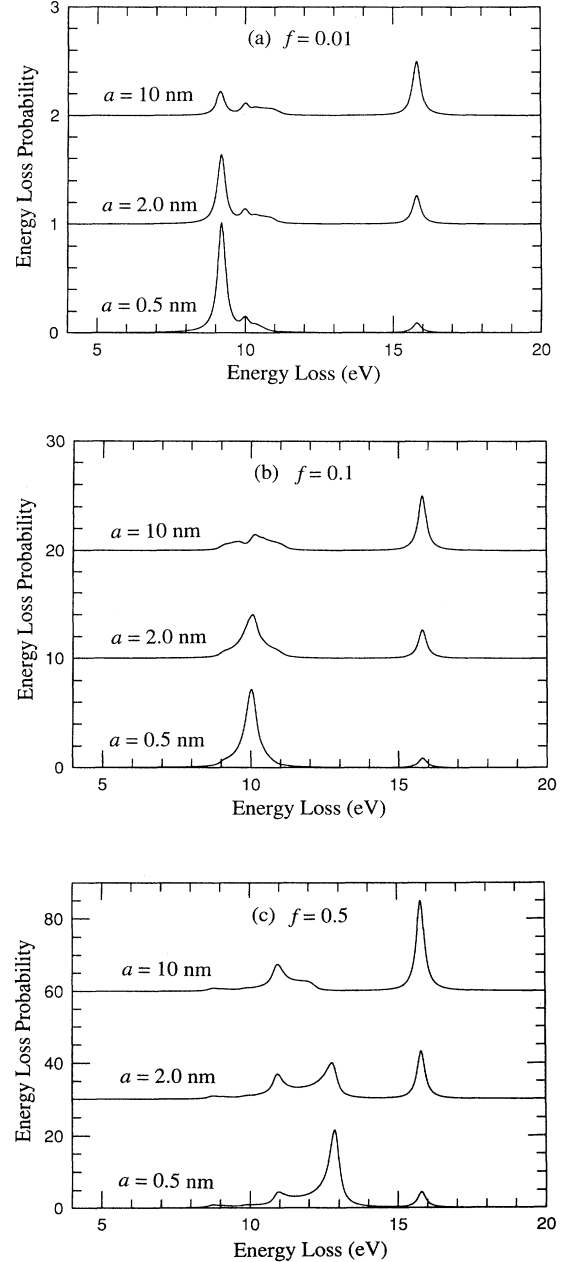

FIG. 5. Energy-loss probability density $\Xi(E)$ for Al spheres in vacuum, as a function of energy loss E, with three values of the sphere radius: $a = 0.5$, 2.0, and 10.0 nm. $\Xi(E)$ is the dimensionless quantity defined in Eq. (41). Plots (a), (b), and (c) are for sphere volume fractions $f = 0.01$, $f = 0.1$, and $f = 0.5$, respectively. The incident electron energy is 100 KeV. The zero points on the ordinates have been shifted upward for the larger values of a.

tained in Ref. 26, where the case of electron energy loss from a single, isolated sphere in vacuum is treated in detail.

B. Aluminum spheres in vacuum

We now use Eq. (41) to calculate the energy-loss spectrum for a simple model system of aluminum spheres in a vacuum host, using a free-electron dielectric function for the aluminum, $\varepsilon_1 = 1 - (\omega_p)^2 / [\omega(\omega + i\gamma)]$, where $\hbar\omega_p = 15.8$ eV. The damping factor $\gamma = 0.02\omega_p$ is chosen arbitrarily so as to make the peaks in the energy-loss spectrum easily visible, and is, in fact, about one-half as large as in actual aluminum.[27] The incident electron energy is $E_I = 100$ KeV. Figures 5(a), 5(b), and 5(c) show the energy-loss spectrum for three values of the volume fraction: $f = 0.01$, 0.1, and 0.5. For each volume fraction, three different sphere radii are chosen: $a = 0.5$, 2.0, and 10.0 nm.

These three figures show loss peaks in the range 8–13 eV that are associated with surface modes, and a peak at 15.8 eV that is associated with the bulk mode. The important effect of changing the sphere radius is that in the integration over Q, the high-ka modes are weighted more strongly as the radius increases. This has two consequences. First, since the total strength of the surface modes decreases and the strength of the bulk mode increases with increasing ka, as shown in Fig. 1, the total height of the surface mode loss peaks decreases, and the height of the bulk mode loss peak increases, as the sphere radius increases. The second consequence is a systematic variation of the surface mode positions and heights. For the smallest radius, $a = 0.5$ nm, the most prominent peak is associated with the $s = 1$ surface mode, for small ka, predominantly a dipolar mode, that has the largest strength and exhibits a shift in position as the volume fraction f changes. As f takes on the values 0.01, 0.1, and 0.5, this peak moves from 9.2 to 10.0 eV and finally to 12.9 eV, energies that are consistent with the values of the depolarization factor for this mode, $n_s = 0.34$, 0.40, and 0.667. As a increases, the height of this dipole peak decreases, and a peak at about 11 eV grows; this is associated with the closely spaced surface modes with depolarization factors in the region between $n_s = 0.45$ and 0.5, whose strength grows with increasing ka. Several other peaks that can be associated with specific surface modes also appear, but we shall not discuss these in detail.

C. Al spheres in AlF$_3$ host

Howie and Walsh[15] found that if a high-intensity beam of electrons is focused on a thin sample of AlF$_3$, a small hole can be drilled in the sample. Colloidal Al particles are formed in the region immediately surrounding the hole, as indicated by the appearance of Al bulk and interface loss peaks in the electron-energy-loss spectrum, when electrons pass through this region. If the electrons pass through the hole which has been drilled previously, the interface loss peak still persists but the Al bulk loss peak is missing.

Howie and Walsh[15] proposed a model, based on classi-

cal electron trajectories, which they used to explain the data qualitatively. They calculated an inverse effective dielectric function, whose imaginary part gave bulk loss peaks in both Al and AlF$_3$, as well as interface loss peaks. They showed how the heights of these peaks varied with the Al volume fraction f and the radius a of the spherical Al particles. Because of the simplicity of model, they did not attempt to fit the data precisely, nor did they find values of f and a.

We have used Eq. (41) to calculate the energy-loss spectrum $\Xi(E)$ for this system, allowing f and a to vary so as to give the best fit with the experiment. For Al we took a free-electron dielectric function $\varepsilon_1 = 1 - (\omega_p)^2 / [\omega(\omega + i\gamma)]$, where $\hbar\omega_p = 15.8$ eV, and the damping factor is $\gamma = \gamma_b + \gamma_s$. Here $\gamma_b = 0.04\omega_p$ is the experimental bulk damping factor for Al and the second term, $\gamma_s = v_f / a$ represents a contribution from surface scattering, or from an alternate point of view, a width parameter that is caused by the distribution of surface plasmon excitations over a large number of quantized energy levels in a small sphere.[27,28] The surface damping term γ_s can be comparable to the bulk damping term for small spheres. For example, if $a = 2.6$ nm, then $\gamma_s = 0.032$. The dielectric function of AlF$_3$ was found by Howie and Walsh[29] from an analysis of the electron-energy-loss spectrum of pure AlF$_3$.

The experimental curve, shown by the dashed line in Fig. 6, was normalized so that the areas under the experimental and theoretical curves were equal. The broad peak at 25 eV is the bulk plasmon loss peak for AlF$_3$, the narrower peak at 15.8 eV is the bulk plasmon loss peak for Al, and the peak at 8.5 eV is the interface loss peak. The parameter values for which the agreement between theory and experiment is best are $f = 0.25$ and $a = 2.6$ nm. Increasing the value of f has two effects: (1) The heights of the interface and bulk loss peaks for Al increase, compared to the AlF$_3$ bulk loss; (2) The interface loss peak moves to higher energy. With increasing sphere radius a, the Al bulk loss peak increases whereas the interface loss peak decreases.
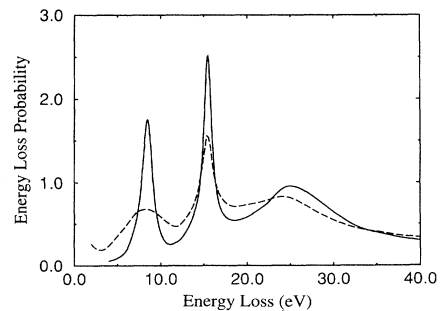
It is evident from Fig. 6 that although the peak posi-

FIG. 6. Energy-loss probability density $\Xi(E)$ for Al spheres of radius $a = 2.6$ nm and volume fraction $f = 0.25$, in an AlF$_3$ host. The incident electron energy is 100 KeV. Dashed line: experiment; solid line: theory.

tions and areas are well described by the theory, the experimental loss peaks are wider than the corresponding theoretical ones. If the bulk damping factor γ_b is increased to about $\gamma_b = 0.1\omega_p$, the theoretical Al bulk loss peak is broadened so that it agrees with the corresponding experimental peak, but the theoretical interface and AlF_3 bulk loss peaks are still too narrow. It is possible that this increased value of γ_b can be attributed to imperfections in the Al spheres. The fact that the theoretical interface loss peak is still too narrow, even when using this larger value of γ_b, may be due to nonspherical particle shapes, a variation of the volume fraction f over the region traversed by the electron beam, or inaccuracy of the mean-field approximation at this relatively large value of f. Radiation damage of the AlF_3 host material may be responsible for the bulk AlF_3 loss peak discrepancy at 25 eV. If one begins with pure AlF_3, and a volume fraction $f = 0.25$ of colloidal Al is formed as a result of the electron irradiation, the remaining AlF_3 must be altered significantly, and it is unlikely that its dielectric function can be represented adequately with that of pure AlF_3. An attempt to model the host material as a mixture of bulk AlF_3 and vacuum-filled voids gave better agreement between theory and experiment in the 20–30 eV energy range, but did not improve the overall agreement over the entire energy range.

IV. SUMMARY

The theory of energy loss for fast electrons passing through a single particle of various sizes and shapes has been thoroughly described in the literature. However, if a system contained many randomly located particles, no formalism existed for including interactions between the particles and averaging over the positions of the particles. We have approached this problem by calculating $\varepsilon^{-1}(k,\omega)$, the effective inverse longitudinal dielectric function of a system containing identical spherical particles with local dielectric function $\varepsilon_1(\omega)$, randomly located in a host medium with dielectric function $\varepsilon_2(\omega)$. If one knows $\varepsilon^{-1}(k,\omega)$, the energy-loss probability can be calculated using the first Born approximation.

We were able to find an exact formal expression for $\varepsilon^{-1}(k,\omega)$ that includes interactions of all multipolar orders between the spheres, as well as a configuration average over the random positions of the spheres. Furthermore, $\varepsilon^{-1}(k,\omega)$ can be written in the form of a spectral representation: it is equal to a sum of terms with simple poles and residues that are related, respectively, to the energies and strengths of the normal modes of the system. The positions of these poles and the values of the residues are independent of the materials; they depend only on the wave vector k and on the geometrical microstructure of the system.

In the mean-field approximation, the positions and strengths of the modes can be calculated in terms of f, the volume fraction of the spherical particles, and $\rho^{(2)}(r)$, the two-particle distribution function. As a simple example, we used an excluded volume expression for $\rho^{(2)}(r)$, and found the mode positions and strengths as functions of f and ka. In the local ($k \to 0$) limit, only the dipole in-

terface mode is present, and $\varepsilon^{-1}(k,\omega)$ reduces to the inverse of the Maxwell-Garnett dielectric function. As ka increases, a bulk mode and higher-multipolar interface modes appear. An important feature of the spectral representation is that these statements about the mode behavior can be made independently of the materials.

To illustrate an application of our theory for $\varepsilon^{-1}(k,\omega)$, we calculated the energy-loss probability function for a system of aluminum spheres in vacuum. For a fixed incident electron energy, we presented results showing how the loss peaks varied when f and a were changed, and were able to explain these changes in terms of the behavior of the mode positions and strengths in the spectral representation for $\varepsilon^{-1}(k,\omega)$. Finally, we used our theory to explain the experimental electron-energy-loss spectrum for Al particles in an AlF_3 host. Three loss peaks associated with excitations of interface modes and bulk plasmon modes for Al and AlF_3 are observed. By appropriate choices of the parameters f and a in our theory, we were able to fit the positions and areas of the observed peaks. We also gave possible explanations for the fact that the experimental loss peaks are broader than the theoretical peaks.

APPENDIX A: DETERMINATION OF M_l

We apply an external potential $V^{ext}(\mathbf{r}) = V_0 e^{ikz}$ to a sphere of radius a with dielectric constant ε surrounded by vacuum, and with the sphere center at $\mathbf{r}_i$. After determining the induced potential $v_i^{ind,0}(\mathbf{r})$ both inside and outside the sphere, we can find the kth Fourier component, $V_i^{ind,0}(k)$. The coefficients M_l are defined by Eq. (23).

Introducing a relative coordinate $\mathbf{r}' = \mathbf{r} - \mathbf{r}_i$, we write the external potential

$$V^{ext}(\mathbf{r}) = e^{ikz_i} \widetilde{V}^{ext}(\mathbf{r}') , \tag{A1}$$

where[30]

$$\widetilde{V}^{ext}(\mathbf{r}') = V_0 e^{ikz'}$$

$$= V_0 \sum_{l=0}^{\infty} i^l \sqrt{4\pi(2l+1)} j_l(kr') Y_{l0}(\theta') . \tag{A2}$$

The total potential has the form

$$V_i^0(\mathbf{r}) = \left[\frac{\widetilde{V}^{\text{ext}}(\mathbf{r}')}{\varepsilon} + \sum_{l=0}^{\infty} c_l (r')^l Y_{l0}(\theta') \right] e^{ikz_i}, \quad r' < a$$

$$= \left[\widetilde{V}^{\text{ext}}(\mathbf{r}') + \sum_{l=0}^{\infty} b_l (r')^{-l-1} Y_{l0}(\theta') \right] e^{ikz_i}, \quad r' > a .$$

$$(A3)$$

The unknown coefficients c_l and b_l are determined by requiring that the potential $V_i^0(\mathbf{r})$ and the radial component of the displacement be continuous at $r = a$. Solving the two continuity equations for c_l and b_l, we find, for $l \neq 0$,

$$b_l = -V_0 a^{l+1} \widetilde{\alpha}_l i^l \sqrt{4\pi(2l+1)} j_l(ka) , \quad (A4)$$

$$c_l = -\varepsilon^{-1}[(l+1)/l]a^{-2l-1}b_l , \quad (A5)$$

where

$$\widetilde{\alpha}_l = \frac{l(\varepsilon-1)}{l(\varepsilon+1)+1} = \frac{n_l^0}{(\varepsilon-1)^{-1}+n_l^0} \quad (A6)$$

is the dimensionless l polarizability for the l multipole of the sphere, the actual polarizability being

$$\alpha_l = a^{2l+1}\widetilde{\alpha}_l . \quad (A7)$$

In Eq. (A6), $n_l^0 = l/(2l+1)$. Equations (A4) and (A5) are not valid if $l = 0$. Instead, we have $b_0 = 0$ and

$$c_0 = V_0[(\varepsilon-1)/\varepsilon]a^{-1}i\sqrt{4\pi}j_0(ka) . \quad (A8)$$

The induced potential is found by subtracting the external potential [Eq. (A1)] from the total potential [Eq. (A3)], giving

$$V_i^{\text{ind},0}(\mathbf{r}) = \left[\widetilde{V}^{\text{ext}}(\mathbf{r}')\left[\frac{1}{\varepsilon}-1\right] \right.$$

$$\left. + \sum_{l=0}^{\infty} c_l (r')^l Y_{l0}(\theta') \right] e^{ikz_i}, \quad r' < a$$

$$= \left[\sum_{l=1}^{\infty} b_l (r')^{-l-1} Y_{l0}(\theta') \right] e^{ikz_i}, \quad r' > a . \quad (A9)$$

The Fourier expansion of a function $F(\mathbf{r})$ is

$$F(\mathbf{r}) = \sum_k F(k)e^{ikz} , \quad (A10)$$

and the inverse of Eq. (A10) is

$$F(k) = v^{-1}\int d^3r\, F(\mathbf{r})e^{-ikz} . \quad (A11)$$

To find the kth Fourier component of the induced potential, $V_i^{\text{ind},0}(k)$, we replace $F(\mathbf{r})$ by $V_i^{\text{ind},0}(\mathbf{r})$ in Eq. (A11), write $e^{-ikz} = e^{-ikz_i}e^{-ikz'}$, and use the complex conjugate of Eq. (A2) to expand $e^{-ikz'}$. The result is

$$V_i^{\text{ind},0}(k) = v^{-1}\int d^3r' \sum_{l'} (-i)^{l'}\sqrt{4\pi(2l'+1)}$$

$$\times j_{l'}(kr')Y_{l'0}(\theta')V_i^{\text{ind},0}(\mathbf{r})e^{-ikz_i} . \quad (A12)$$

After substituting the expression for $V_i^{\text{ind},0}(\mathbf{r})$ from Eq. (A9) into Eq. (A12), the integration over θ' and ϕ', with the orthonormality of $Y_{l0}(\theta',\phi')$ and $Y_{l'0}(\theta',\phi')$, gives the single term $l' = l$ in the sum over l'. The r' integration can be done using[31]

$$\int_0^a r^{l+2}j_l(kr)dr = k^{-1}a^{l+2}j_{l+1}(\rho) , \quad (A13)$$

$$\int_a^\infty r^{1-l}j_l(kr)dr = k^{-1}a^{1-l}j_{l-1}(\rho) , \quad l \geq 1 , \quad (A14)$$

where $\rho = ka$, and

$$\int_0^a r^2[j_l(kr)]^2 dr \equiv \frac{1}{2}a^2 S_l(\rho) \quad (A15)$$

with

$$S_l(\rho) = [j_l(\rho)]^2 - j_{l-1}(\rho)j_{l+1}(\rho) , \quad l \geq 1$$

$$= [j_0(\rho)]^2 + n_0(\rho)j_1(\rho) , \quad l = 0 , \quad (A16)$$

where $n_0(\rho) = -\rho^{-1}\cos\rho$.

We find that Eq. (A12) can be written in the form of Eq. (23), so the final result for the coefficients M_l is

$$M_l = \frac{4\pi a^3}{v}(2l+1)\left\{ \frac{1}{2}\left[\frac{1}{\varepsilon}-1\right]S_l(\rho) - \widetilde{\alpha}_l\left[-\frac{l+1}{\varepsilon l}j_{l+1}(\rho)+j_{l-1}(\rho)\right]\frac{j_l(\rho)}{\rho} \right\}, \quad l \geq 1$$

$$= \frac{4\pi a^3}{v}\left[\frac{1}{\varepsilon}-1\right]\left\{ \frac{1}{2}S_0(\rho)-\frac{1}{\rho}j_1(\rho)j_0(\rho) \right\}, \quad l = 0 .$$

$$(A17)$$

APPENDIX B: DETERMINATION OF F_l

The same external potential $V^{\text{ext}}(\mathbf{r}) = V_0 e^{ikz}$ is applied to sphere i as in Appendix A. Multipole moments q_{li}^0 proportional to the amplitude V_0 are induced on the sphere, and the constants of proportionality F_l are defined in Eq. (12).

The induced potential outside the sphere is used to define the multipole moment. For a general multipole q_{lm} located at the origin, the potential is

$$V(\mathbf{r}) = \sum_{lm} \frac{4\pi}{2l+1}q_{lm}r^{-l-1}Y_{lm}(\theta,\varphi) . \quad (B1)$$

Applying this equation to the present situation, where the induced multipoles have $m=0$ and $\mathbf{r}$ must be replaced by the relative position vector $\mathbf{r}'$, we get

$$V_i^{\text{ind},0}(\mathbf{r}') = \sum_{l=1}^{\infty} \frac{4\pi}{2l+1} q_{li}^0 (r')^{-l-1} Y_{l0}(\theta') , \quad r' > a . \quad \text{(B2)}$$

Comparing Eqs. (B2) and (A9), we find

$$q_{li}^0 = \frac{2l+1}{4\pi} b_l e^{ikz_i} . \quad \text{(B3)}$$

Substitution of Eq. (A4) for the coefficient b_l into Eq. (B3) and comparison with Eq. (12) gives the result

$$F_l = -a^{l+1} \tilde{\alpha}_l i^l (4\pi)^{-1/2} (2l+1)^{3/2} j_l(\rho) . \quad \text{(B4)}$$

$$V(\mathbf{r}) = V^e(\mathbf{r}) + V_i^{\text{ind},1}(\mathbf{r})$$

$$= \sum_{lm} V_{lmi}(r')^l Y_{lm}(\theta',\varphi') + \sum_{lm} c_{lm}(r')^l Y_{lm}(\theta',\varphi') , \quad r' < a$$

$$= \sum_{lm} V_{lmi}(r')^l Y_{lm}(\theta',\varphi') + \sum_{lm} b_{lm}(r')^{-l-1} Y_{lm}(\theta',\varphi') , \quad r' > a . \quad \text{(C2)}$$

From the continuity of the potential and the radial component of the displacement at $r=a$, we can solve for the unknown coefficients b_{lm} and c_{lm}:

$$b_{lm} = -\alpha_l V_{lmi} = \frac{4\pi}{2l+1} q_{lmi}^1 , \quad \text{(C3)}$$

$$c_{lm} = -\tilde{\alpha}_l V_{lmi} , \quad \text{(C4)}$$

where the second equality in Eq. (C3) has been found by comparing the terms containing b_{lm} in Eqs. (C2) with Eq. (B1).

Finally, the kth Fourier component of $V_i^{\text{ind},1}(\mathbf{r})$ (the terms in Eq. (C2) that contain b_{lm} and c_{lm}) is

$$V_i^{\text{ind},1}(k) = v^{-1} \int d^3 r e^{-ikz'} V_i^{\text{ind},1}(\mathbf{r}') e^{-ikz_i} . \quad \text{(C5)}$$

We expand $e^{-ikz'}$ as in Eq. (A12), and the resulting integrations can be carried out in the same way as in Appendix A. From the orthogonality of the spherical harmonics, only the $m=0$ terms in Eq. (C2) contribute to $V_i^{\text{ind},1}(k)$. The identity

APPENDIX C: DETERMINATION OF Z_l

Consider sphere i, acted on by the potential $V^e(\mathbf{r})$ from other spheres $j \neq i$. This potential induces multipoles q_{lmi}^1 on sphere i, and all these multipoles q_{li}^1 (with $m=0$) produce an induced potential $V_i^{\text{ind},1}(\mathbf{r})$. The kth Fourier component of $V_i^{\text{ind},1}(\mathbf{r})$ is $V_i^{\text{ind},1}(k)$, which is proportional to q_{li}^1, the constants of proportionality being Z_l, as defined in Eq. (24).

The potential $V^e(\mathbf{r})$ can be expanded about the center of sphere i:

$$V^e(\mathbf{r}) = \sum_{lm} V_{lmi}(r')^l Y_{lm}(\theta',\varphi') , \quad \text{(C1)}$$

where the coefficients V_{lmi} carry the phase factor e^{ikz_i}. $V^e(\mathbf{r})$ is considered as an external potential acting on the sphere, so the total potential is the sum of $V^e(\mathbf{r})$ and the unknown induced potential $V_i^{\text{ind},1}(\mathbf{r})$:

$$j_{l+1}(\rho) + j_{l-1}(\rho) = (2l+1) j_l(\rho)/\rho \quad \text{(C6)}$$

is useful for simplifying the equations. We find

$$V_i^{\text{ind},1}(k) = -v^{-1} \sum_{l=1}^{\infty} (-i)^l \sqrt{4\pi} (2l+1)^{3/2}$$

$$\times k^{-2} a^{-l} j_l(ka) \alpha_l V_{li} e^{-ikz_i} . \quad \text{(C7)}$$

If we express $\alpha_l V_{li}$ in terms of q_{li}^1 using Eqs. (C3) and compare Eq. (C7) with Eq. (24), we get

$$Z_l = v^{-1}(-i)^l 4\pi \sqrt{4\pi(2l+1)} k^{-2} a^{-l} j_l(\rho) . \quad \text{(C8)}$$

APPENDIX D: MULTIPOLAR INTERACTION

1. Determination of $H_{ll'}$

In this appendix the missing steps in the derivations leading from Eq. (15) to Eq. (20) are filled in. The coefficients $B_{lmi}^{l'm'j}$ that appear in Eq. (15) are[21]

$$B_{lmi}^{l'm'j} = (-1)^{l'+m'} \frac{Y_{l+l',m-m'}(\theta_{ij},\varphi_{ij})^*}{(r_{ij})^{l+l'+1}} \left[\frac{(4\pi)^3 (l+l'+m-m')!(l+l'-m+m')!}{(2l+1)(2l'+1)(2l+2l'+1)(l+m)!(l-m)!(l'+m')!(l'-m')!} \right]^{1/2} , \quad \text{(D1)}$$

where r_{ij} is the distance between spheres i and j, and $(\theta_{ij},\varphi_{ij})$ are the polar and azimuthal angles of sphere j with respect to sphere i. Note that $B_{lmi}^{l'm'j}$ is a complex Hermitian matrix; the various substitutions that will be

made in the derivation below have been chosen so that the final matrix $H_{ll'}$, which has to be diagonalized is real and symmetric. Its eigenvalues are the depolarization factors that appear in the spectral representation.

Beginning with Eq. (16), we introduce new variables y_{lmi} and $y_{l'm'j}$ defined by Eq. (18), multiply both sides by $(-i)^l[(2l+1)\alpha_l]^{-1}\sqrt{l}a^{2l+1}e^{-ikz}$, and write the l polarizability α_l using the second form in Eq. (A6). We also express q_{li}^0, on the right-hand side of Eq. (16), as

$$q_{li}^0=F_lV_0e^{ikz_i}=-[(2l+1)/4\pi]\alpha_lV_0R_le^{ikz_i} , \qquad (D2)$$

where [by comparing Eq. (D2) with Eq. (B3) for F_l], we have

$$R_l=(i/a)^l\sqrt{4\pi(2l+1)}j_l(\rho) . \qquad (D3)$$

Making these substitutions, we can write Eq. (16) in the form of Eq. (17), where

$$h_{lmi}^{l'm'j}=(4\pi)^{-1}\sqrt{ll'}a^{2l+1}a^{2l'+1}\overline{B}_{lmi}^{l'm'j}e^{ik(z_j-z_i)} , \qquad (D4)$$

with

$$\overline{B}_{lmi}^{l'm'j}=(-i)^l(i)^{l'}B_{lmi}^{l'm'j} . \qquad (D5)$$

We use mean-field theory to go from Eq. (17) to Eq. (19), setting $m=m'=0$ (simply omitting the m,m' indices) and replacing the multipole variables y and the h

matrix by ensemble averages. The B matrix in Eq. (D1) simplifies, and so the average h matrix in Eq. (19) is

$$\left\langle\sum_j h_{li}^{l'j}(k)\right\rangle=(4\pi)^{-1}\sqrt{ll'}a^{l+l'+1}\left\langle\sum_j \overline{B}_{li}^{l'j}e^{ik(z_j-z_i)}\right\rangle , \qquad (D6)$$

where

$$\overline{B}_{li}^{l'j}=(-i)^l(i)^{l'}\gamma_{ll'}Y_{l+l',0}(\theta_{ij})^*/(r_{ij})^{l+l'+1} , \qquad (D7)$$

with

$$\gamma_{ll'}=(-1)^{l'}\left\{\frac{(4\pi)^3[(l+l')!]^2}{(2l+1)(2l'+1)(2l+2l'+1)(l!)^2(l'!)^2}\right\}^{1/2} . \qquad (D8)$$

The ensemble averaged sum over j on the right-hand side of Eq. (D6) can be carried out by writing $\mathbf{r}_j-\mathbf{r}_i=\mathbf{r}$, $z_j-z_i=z$, and $\theta_{ij}=\theta$, inserting the two-particle distribution function $\rho^{(2)}(r)$, and replacing the sum over j by an integration over $\mathbf{r}$:

$$\left\langle\sum_j \overline{B}_{li}^{l'j}e^{ik(z_j-z_i)}\right\rangle=(-i)^l(i)^{l'}\gamma_{ll'}\int\rho^{(2)}(r)Y_{l+l',0}(\theta)r^{-(l+l'+1)}e^{ikz}d^3r \qquad (D9)$$

$$=(-i)^l(i)^{l'}\gamma_{ll'}\int\rho^{(2)}(r)\sum_{l''}(i)^{l''}\sqrt{4\pi(2l''+1)}j_{l''}(kr)Y_{l'',0}(\theta)Y_{l+l',0}(\theta)r^{-(l+l'+1)}r^2dr\,d\Omega , \qquad (D10)$$

where we have used Eq. (A2) to expand e^{ikz}. The angular integration gives $\delta_{l+l',l''}$, and so,

$$\left\langle\sum_j \overline{B}_{li}^{l'j}e^{ik(z_j-z_i)}\right\rangle=(-1)^{l'}\gamma_{ll'}\sqrt{4\pi(2l+2l'+1)}$$

$$\times\int_0^\infty \rho^{(2)}(r)\frac{j_{l+l'}(kr)}{r^{l+l'-1}}dr . \qquad (D11)$$

We substitute Eq. (D8) for $\gamma_{ll'}$, and find

$$\left\langle\sum_j \overline{B}_{li}^{l'j}e^{ik(z_j-z_i)}\right\rangle=\frac{(4\pi)^2(l+l')!}{l!(l')!\sqrt{2l+1}(2l'+1)}I_{l+l'}(k) , \qquad (D12)$$

where

$$I_\lambda(k)=\int_0^\infty\rho^{(2)}(r)j_\lambda(kr)r^{1-\lambda}dr . \qquad (D13)$$

Integration by parts gives an alternative form for $I_\lambda(k)$, using the identity $(d/dx)[x^{1-\lambda}j_{\lambda-1}(x)]=-x^{1-\lambda}j_\lambda(x)$ and the fact that $\rho^{(2)}(r)r^{1-\lambda}j_{\lambda-1}(kr)=0$ at $r=0$ and $r=\infty$:

$$I_\lambda(k)=k^{-1}\int_0^\infty[d\rho^{(2)}(r)/dr]j_{\lambda-1}(kr)r^{1-\lambda}dr . \qquad (D14)$$

Finally, combining Eqs. (D6) and (D13), we have

$$\left\langle\sum_j h_{li}^{l'j}(k)\right\rangle=4\pi\sqrt{ll'/(2l+1)(2l'+1)}$$

$$\times\frac{(l+l')!}{l!(l')!}a^{l+l'+1}I_{l+l'}(k) \qquad (D15)$$

and $H_{ll'}$ is defined as

$$H_{ll'}=n_l^0\delta_{ll'}+\left\langle\sum_j h_{li}^{l'j}(k)\right\rangle , \qquad (D16)$$

with $n_l^0=l/(2l+1)$.

2. Solution for the multipole moments

The matrix $H_{ll'}$ which we have found in Eq. (D16) appears in Eq. (19), which we can rewrite as

$$\sum_{l'}[(\varepsilon-1)^{-1}\delta_{ll'}+H_{ll'}]\langle y_{l'}\rangle=T_l , \qquad (D17)$$

where the quantity T_l stands for the right-hand side of Eq. (19). If the eigenvalues of $H_{ll'}$ are n_s and the eigenvectors are the columns of a matrix U, the transformation which diagonalizes H is

$$\sum_{ll'}U_{sl}^{-1}H_{ll'}U_{l's'}=n_s\delta_{ss'} . \qquad (D18)$$

Multiplying Eq. (D17) by the matrix U on the left and inserting $U^{-1}U$ between the square bracket and $\langle y_{l'}\rangle$, we find the solution

$$\langle y_l\rangle=\sum_{l'}G_{ll'}T_{l'} \qquad (D19)$$

with

$$G_{ll'}=\sum_s\frac{U_{ls}U_{sl'}^{-1}}{(\varepsilon-1)^{-1}+n_s} . \qquad (D20)$$

Finally, we use Eqs. (17) and (D19) to solve for $\langle q_{li} \rangle$ and substitute the right-hand side of Eq. (19) for T_j. The result is Eq. (20), where

$$D_{ll'}(s) = -(4\pi)^{-1} i^l (-i)^{l'} \sqrt{ll' a^{2l+1} a^{2l'+1}} U_{ls} U_{l's} .$$

(D21)

In the derivation of Eq. (D21) we also have used the equality $U_{sl'}^{-1} = U_{l's}$ (i.e., U is a real orthogonal matrix), which follows from the fact that $H_{ll'}$ is a real symmetric matrix.

APPENDIX E: SPECTRAL REPRESENTATION

In this appendix the derivation of Eq. (27) starting from Eq. (26) is discussed. The volume fraction of spheres is $f = \frac{4}{3}\pi a^3 N/v$, so we can write $N = f v/\frac{4}{3}\pi a^3$ in Eq. (26). If we also introduce the spectral variable $u = -1/(\varepsilon - 1)$, the expression for the inverse dielectric function is

$$\varepsilon^{-1}(k,\omega) = 1 + (f v/\frac{4}{3}\pi a^3) \left[\sum_{l=0}^{\infty} (M_l - Z_l F_l) - \sum_{sll'} \frac{Z_l D_{ll'}(s) R_{l'}}{u - n_s} \right] . \qquad (E1)$$

Combining the expressions for Z_l [Eq. (C8)] and F_l [Eq. (B4)], one finds

$$Z_l F_l = -(4\pi a^3/v)(2l+1)^2 \tilde{\alpha}_l [j_l(\rho)/\rho]^2 . \qquad (E2)$$

Equation (E1) has terms containing denominators of three kinds: $u - 1$, $u - n_l^0 = u - l/(2l+1)$, and $u - n_s$, which are of interest since a zero denominator corresponds to a resonant mode of the system.

(a) The denominator $u - 1$, corresponding to the bulk longitudinal mode, comes from two terms in M_l, one containing $(\varepsilon^{-1} - 1)$ and the other, $\tilde{\alpha}_l/\varepsilon$. [See Eq. (A6) for $\tilde{\alpha}_l$ and Eq. (A17) for M_l.]

(b) The denominator $u - n_l^0$, corresponding to a surface mode of an isolated sphere, comes from all terms that contain $\tilde{\alpha}_l$: from M_l where there are both $\tilde{\alpha}_l/\varepsilon$ and $\tilde{\alpha}_l$ terms, and also from $Z_l F_l$, which is proportional to $\tilde{\alpha}_l$.

(c) The denominators $u - n_s$, corresponding to surface modes of the coupled system of spheres, appear in the second sum in Eq. (E1).

It can be shown, using the identity in Eq. (C6), that the terms in $M_l - Z_l F_l$ containing the denominator $u - n_l^0$ cancel. This is responsible physically since the spheres are, in fact, coupled with each other, so we do not expect any resonances corresponding to surface modes of an isolated sphere. Therefore, we find

$$\sum_{l=0}^{\infty} (M_l - Z_l F_l) = (4\pi a^3/v) \sum_{l=0}^{\infty} (2l+1)[\tfrac{1}{2}S_l(\rho) - j_{l+1}(\rho)j_l(\rho)/\rho] \frac{1}{u-1} \qquad (E3)$$

$$= (\tfrac{4}{3}\pi a^3/v) \frac{C_b}{u-1} , \qquad (E4)$$

where

$$C_b = 3 \sum_{l=0}^{\infty} (2l+1)[\tfrac{1}{2}S_l(\rho) - j_{l+1}(\rho)j_l(\rho)/\rho] . \qquad (E5)$$

Using expressions for Z_l, [Eq. (C8)], $D_{ll'}(s)$ [Eq. (D18)], and R_l [Eq. (D3)], we can write the numerator in the second sum in Eq. (E1) in the form

$$Z_l D_{ll'}(s) R_l = -(4\pi a^3/v) C_{ll'}(s) , \qquad (E6)$$

where

$$C_{ll'}(s) = 3\sqrt{ll'(2l+1)(2l'+1)} \rho^{-2} j_l(\rho) j_{l'}(\rho) U_{ls} U_{sl'}^{-1} . \qquad (E7)$$

After substitution of Eqs. (E4) and (E6), Eq. (E1) takes on the simple form

$$\varepsilon^{-1}(k,\omega) = 1 + f \left[\frac{C_b}{u-1} + \sum_s \frac{C_s}{u - n_s} \right] , \qquad (E8)$$

where

$$C_s = \sum_{ll'} C_{ll'}(s) \qquad (E9)$$

is the surface mode strength given by Eq. (32), and C_b is the bulk mode strength given by Eq. (E5), which can still be simplified. By substituting Eq. (A15) for $S_l(\rho)$, one can show,

$$\frac{3}{2} \sum_{l=0}^{\infty} (2l+1) S_l(\rho) = \frac{3}{2} \sum_{l=0}^{\infty} (2l+1) \frac{2}{a^3} \int_0^a r^2 [j_l(kr)]^2 dr$$

$$= \frac{3}{a^3} \int_0^a r^2 \left\{ \sum_{l=0}^{\infty} (2l+1)[j_l(kr)]^2 \right\} dr$$

$$= \frac{3}{a^3} \int_0^a r^2 \left\{ \sum_{l=0}^{\infty} (2l+1) \frac{\pi}{2kr} \left[J_{l+\frac{1}{2}}(kr) \right]^2 \right\} dr = 1 , \qquad (E10)$$

since the quantity in the curly brackets has the value 1.[32] Then using the identity (C6) one can demonstrate that

$$\sum_{l=0}^{\infty}(2l+1)\rho^{-1}j_{l+1}(\rho)j_l(\rho)=\sum_{l=1}^{\infty}l(2l+1)\left[\frac{j_l(\rho)}{\rho}\right]^2 .$$

(E11)

Therefore, combining Eqs. (E5), (E10), and (E11) one gets the expression for C_b given in Eq. (29).

The spectral representation (E8) applies to spheres with dielectric function ε surrounded by vacuum. The spectral representation in Eq. (27), which applies to the system with dielectric functions ε_1 and ε_2 for the spheres and host, respectively, is found from Eq. (E8) by making the substitutions described in the discussion after Eq. (28). This procedure also changes the spectral variable u, defined above Eq. (E1), to the quantity defined by Eq. (28).

APPENDIX F: SUM RULES

1. Mean-field theory

We first prove the sum rule in Eq. (33), which states that the total strength of all modes is 1. From Eqs. (E7) and (E9), using the fact that $\sum_s U_{ls}U_{sl'}^{-1}=\delta_{ll'}$, one finds the total strength of the surface modes:

$$\sum_s C_s=\sum_{sll'}C_{ll'}(s)=3\sum_{l=1}^{\infty}l(2l+1)[j_l(\rho)/\rho]^2 .$$

(F1)

Then using Eq. (29), the sum rule in Eq. (33) follows immediately.

Next, we prove the sum rule in Eq. (34) for the first moment of the surface modes, $\sum_s C_s n_s$. We use Eqs. (E7) and (E9) for C_s, and write $n_s=\sum_{s'}n_s\delta_{ss'}$. This gives

$$\sum_s C_s n_s=\sum_{sll'}C_{ll'}(s)n_s$$

$$=\sum_{ss'll'}3\sqrt{ll'(2l+1)(2l'+1)}\rho^{-2}j_l(\rho)$$

$$\times j_{l'}(\rho)U_{ls}U_{s'l'}^{-1}n_s\delta_{ss'} .$$

(F2)

Inverting Eq. (D18), we have $\sum_{ss'}U_{ls}n_s\delta_{ss'}U_{s'l'}^{-1}=H_{ll'}$, and so Eq. (F2) becomes

$$\sum_s C_s n_s=\sum_{ll'}3\sqrt{ll'(2l+1)(2l'+1)}\rho^{-2}j_l(\rho)j_{l'}(\rho)H_{ll'} .$$

(F3)

2. Exact theory

The spectral representation in Eq. (27), derived using mean-field theory, is a special case of a more general spectral representation,

$$\varepsilon^{-1}(k,\omega)=(\varepsilon_2)^{-1}\left[1+f\int\frac{g(n)dn}{u-n}\right] ,$$

(F4)

where the exact spectral function $g(n)$ can be written as the sum of two terms,

$$g(n)=C_b\delta(n-1)+g_{sm}(n) .$$

(F5)

The first term corresponds to the bulk longitudinal mode, whereas the second term $g_{sm}(n)$ is a continuous function corresponding to the surface modes of the system of interacting spheres. [Note that in the special case of mean-field theory, the spectral function for the surface modes breaks into a sum of discrete terms, $g_{sm}(n)=\sum_s C_s\delta(n-n_s)$, so Eq. (F4) reduces to Eq. (27).]

We shall find an exact formal expression for $g_{sm}(n)$, from which we can derive a sum rule stating that the exact total strength of the surface modes equals the total strength of these modes in mean-field theory.

$$\int g_{sm}(n)dn=\sum_s C_s=3\sum_{l=1}^{\infty}l(2l+1)[j_l(\rho)/\rho]^2 .$$

(F6)

We also will show that C_b, the strength of the bulk mode, is given correctly by Eq. (29), a result that is independent of the volume fraction and spatial distribution of the spheres. This proves the general sum rule

$$\int g(n)dn=C_b+\int g_{sm}(n)dn=1 .$$

(F7)

Although we shall prove the sum rule in Eq. (F7) explicitly for a system containing identical spherical particles, it actually holds for any two-component system, irrespective of the shapes and sizes of the particles, since it is equivalent to the f-sum rule. This can be shown most easily by considering the high-frequency asymptotic behavior of Eq. (F4).[33] If the individual components satisfy the f-sum rule, then to order ω^{-2}, $[\varepsilon_1(\omega)]^{-1}\rightarrow1+(\omega_{p1})^2/\omega^2$ and $[\varepsilon_2(\omega)]^{-1}\rightarrow1+(\omega_{p2})^2/\omega^2$, whereas for the composite system, $\varepsilon^{-1}(k,\omega)\rightarrow1+(\Omega_p)^2/\omega^2$, where the plasma frequency squared of the composite system is a weighted average of the squares of the plasma frequencies of the two components, $(\Omega_p)^2=f(\omega_{p1})^2+(1-f)(\omega_{p2})^2$. Taking these high-frequency limits in Eq. (F4), one can prove the sum rule (F7).

A second sum rule states that the centroid of the spectral function $\bar{n}_{sm}$ is given correctly by mean-field theory:

$$\bar{n}_{sm}\equiv\frac{\int ng_{sm}(n)dn}{\int g_{sm}(n)dn}=\frac{\sum_s C_s n_s}{\sum_s C_s} .$$

(F8)

We begin with Eq. (18), which describes the coupling between multipoles on an arbitrarily large number of spheres. Denoting the right-hand side of Eq. (18) by t_{lmi} and defining $H_{lmi}^{l'm'j}=n_l^0\delta_{ll'}\delta_{mm'}\delta_{ij}+h_{lmi}^{l'm'j}(k)$, this equation can be written

$$\sum_{l'm'j}[(\varepsilon-1)^{-1}+H_{lmi}^{l'm'j}]y_{l'm'j}=t_{lmi} .$$

(F9)

The method for solving Eq. (F9) is similar to that presented in Eqs. (D17)–(D20). Denoting exact quantities by a caret symbol $^\wedge$, we note that $\hat{n}_s$, the exact depolarization factors of the surface modes, are eigenvalues of $H_{lmi}^{l'm'j}$, and so,

$$\sum_{lmi,l'm'j}\hat{U}_{s,lmi}^{-1}H_{lmi}^{l'm'j}\hat{U}_{l'm'j,s'}=\hat{n}_s\delta_{ss'} .$$

(F10)

Solving Eq. (F9) for y_{lmi}, we find

$$y_{lmi} = \sum_{l'm'j} \hat{G}_{lmi,l'm'j} t_{l'm'j} , \tag{F11}$$

where

$$\hat{G}_{lmi,l'm'j} = \sum_s \frac{\hat{U}_{lmi,s} \hat{U}_{s,l'm'j}^{-1}}{(\varepsilon-1)^{-1} + \hat{n}_s} . \tag{F12}$$

Next, the multipoles q_{l0i} are found from y_{l0i} using Eq. (18), and Eq. (24) gives $V_i^{\text{ind},1}(k)$. [Note that only $m=0$ multipoles contribute.] Also, $m=0$ in t_{lmi}, which stands for the right-hand side of Eq. (17), restricting the sum in Eq. (F11) to $m'=0$. That is, only $m=m'=0$ terms are needed in Eqs. (F11) and (F12). Substituting q_{l0i} into Eq. (25), we find

$$V_i^{\text{ind}}(k) = \left[\sum_{l=0}^{\infty} (M_l - Z_l F_l) + \sum_{sll'j} \frac{Z_l \hat{D}_{l0i,l'0j}(s) R_{l'}}{(\varepsilon-1)^{-1} + \hat{n}_s} \right] V_0 , \tag{F13}$$

where

$$\hat{D}_{l0i,l'0j}(s) = -(4\pi)^{-1} i^l (-i)^{l'} \sqrt{ll' a^{2l+1} a^{2l'+1}} \hat{U}_{l0i,s} \hat{U}_{s,l'0j}^{-1} . \tag{F14}$$

Summing Eq. (F13) over i and taking an ensemble average gives $\langle V^{\text{ind}}(k) \rangle$. We find the exact formal expression

$$\varepsilon^{-1}(k,\omega) = 1 + f \left[\frac{\hat{C}_b}{u-1} + \left\langle \sum_s \frac{\hat{C}_s}{u - \hat{n}_s} \right\rangle \right] , \tag{F15}$$

with

$$\hat{C}_s = \sum_{ll'} \hat{C}_{ll'}(s) , \tag{F16}$$

$$\hat{C}_{ll'}(s) = 3\sqrt{ll'(2l+1)(2l'+1)} \rho^{-2}$$

$$\times j_l(\rho) j_{l'}(\rho) N^{-1} \sum_{ij} \hat{U}_{l0i,s} \hat{U}_{s,l'0j}^{-1} . \tag{F17}$$

The strength of the bulk mode, $\hat{C}_b$, which is contained in the first sum in Eq. (F13), does not depend on the interaction between spheres. Therefore $\hat{C}_b = C_b$, the mean-field value [Eq. (29)]. For a large number of spheres, say $N > 10^6$, the even larger number of surface mode depolarization factors will form an essentially continuous distribution, even before taking an ensemble average. Therefore one can define a continuous spectral

function for the surface modes,

$$g_{\text{sm}}(n) = \left\langle \sum_s \hat{C}_s \delta(n - \hat{n}_s) \right\rangle , \tag{F18}$$

so the ensemble averaged sum over modes in Eq. (F15) can be written

$$\left\langle \sum_s \frac{\hat{C}_s}{u - \hat{n}_s} \right\rangle = \int \frac{g_{\text{sm}}(n) dn}{u - n} . \tag{F19}$$

This completes the derivation of the spectral representation in Eqs. (F4) and (F5).

The sum rule (F6) for the total strength of the surface modes can be proved by noting that $\int g_{\text{sm}}(n) dn = \langle \sum_s \hat{C}_s \rangle$, summing Eq. (F16) over s, and using $\sum_s \hat{U}_{l0i,s} \hat{U}_{s,l'0j}^{-1} = \delta_{ll'} \delta_{ij}$ in Eq. (F17).

The derivation of an expression for the first moment of spectral function is similar to that given in Eqs. (F2)–(F3). We use Eqs. (F19), (F16), and F(17) to find

$$\int n g_{\text{sm}}(n) dn = \left\langle \sum_s \hat{C}_s \hat{n}_s \right\rangle$$

$$= \sum_{ll'} 3\sqrt{ll'(2l+1)(2l'+1)} \rho^{-2} j_l(\rho) j_{l'}(\rho) N^{-1}$$

$$\times \left\langle \sum_{ijs} \hat{U}_{l0i,s} \hat{n}_s \hat{U}_{s,l'0j} \right\rangle . \tag{F20}$$

Now, the ensemble-averaged quantity in Eq. (F20) is

$$\left\langle \sum_{ijs} \hat{U}_{l0i,s} \hat{n}_s \hat{U}_{s,l'0j}^{-1} \right\rangle = \left\langle \sum_{ijss'} \hat{U}_{l0i,s} \hat{n}_s \delta_{ss'} \hat{U}_{s',l'0j}^{-1} \right\rangle$$

$$= \left\langle \sum_{ij} H_{l0i}^{l'0j} \right\rangle$$

$$= \sum_i \left[\sum_j n_l^0 \delta_{ll'} \delta_{ij} + \left\langle \sum_j h_{li}^{l'j}(k) \right\rangle \right]$$

$$= N H_{ll'} , \tag{F21}$$

where we have used the inverse of Eq. (F10), Eq. (D16), and the fact that $H_{ll'}$ is independent of i. Therefore, the right-hand sides of Eqs. (F20) and (F3) are the same, showing that

$$\int n g_{\text{sm}}(n) dn = \sum_s C_s n_s . \tag{F22}$$

This proves Eq. (F8), since the numerators and denominators of both sides are equal.

[1]P. E. Batson, Phys. Rev. Lett. **49**, 936 (1982).

[2]C. Colliex, Adv. Opt. Electron. Microsc. **9**, 65 (1984).

[3]R. H. Ritchie and A. Howie, Philos. Mag. A **58**, 753 (1988).

[4]A. Howie and C. A. Walsh, Radiat. Eff. Defects Solids **117**, 169 (1991).

[5]P. M. Echenique and J. B. Pendry, J. Phys. C **8**, 2936 (1975).

[6]A. Garcia Molina, A. Gras Marti, A. Howie, and R. H. Ritchie, J. Phys. C **18**, 5335 (1985).

[7]T. L. Ferrell and P. M. Echenique, Phys. Rev. Lett. **55**, 1526

(1985).

[8]N. Zabala and A. Rivacoba, Ultramicroscopy **35**, 145 (1991).

[9]P. M. Echenique, A. Howie, and D. J. Wheatley, Philos. Mag. B **36**, 335 (1987); R. Rojas, F. Claro, and R. Fuchs, Phys. Rev. B **37**, 6799 (1988).

[10]B. L. Illman, V. E. Anderson, R. J. Warmack, and T. L. Ferrell, Phys. Rev. B **38**, 3045 (1988).

[11]Z. L. Wang and J. M. Cowley, Ultramicroscopy **21**, 347 (1987).

[12]A. Rivacoba, N. Zabala, and P. M. Echenique, Phys. Rev. Lett. **69**, 3362 (1992).

[13]J. B. Pendry and L. M. Moreno, Phys. Rev. B **50**, 5062 (1994).

[14]J. B. Pendry and A. MacKinnon, Phys Rev. Lett. **69**, 2772 (1992).

[15]A. Howie and C. A. Walsh, Microsc. Microanal. **2**, 171 (1991).

[16]F. Fujimoto and K. Komaki, J. Phys. Soc. Jpn. **25**, 1769 (1968).

[17]P. M. Platzman and P. A. Wolff, *Waves and Interactions in Solid State Physics,* Solid State Physics, Suppl. 13 (Academic, New York, 1973).

[18]C. Kittel, *Quantum Theory of Solids* (Wiley, New York, 1963).

[19]D. Bergman, Phys. Rep. **43**, 377 (1978).

[20]G. Milton, J. Appl. Phys. **52**, 5286 (1981).

[21]R. Fuchs and F. Claro, Phys. Rev. B **39**, 3175 (1989).

[22]K. Hinsen and B. U. Felderhof, Phys. Rev. B **46**, 12 955 (1992).

[23]The term "*Begrenzung* effect," describing the reduction of the bulk mode strength due to the finite particle size, appears to have first been used for spherical particles by M. Schmeitz, J. Phys. C **14**, 1203 (1981), and it also was applied to a slab-shaped sample in the work of H. Boersch, G. Gieger, and W. Stickel, Z. Phys. **212**, 130 (1968). The theory of this effect was first given in the seminal paper of R. H. Ritchie, Phys. Rev. **106**, 874 (1957), in a treatment of electron energy loss by a metallic slab. Note, however, that the term "boundary effect" used by Ritchie has a slightly different meaning, since it includes both the reduction of the bulk plasmon loss and the appearance of surface plasmon loss.

[24]J. C. Maxwell Garnett, Philos. Trans. R. Soc. London **203**, 385 (1904).

[25]Writing Eq. (27) in this form was suggested to us by A. Howie.

[26]D. R. Penn and P. Apell, J. Phys. C **16**, 5729 (1983). In order to compare our results with the ones of this reference we used the following relationship: $\lim_{f \to 0} \int F(E)dE = (N/v) \int d^2 q_{\parallel} \int d\omega P(q_{\parallel},\omega)$, where N is the total number of spheres in the volume v and $P(q_{\parallel},\omega)$ is defined by their Eq. (17). Note also that in their Eq. (21) there is a misprint in the last term: $1/\varepsilon(Q,\omega)$ should be replaced by $1/\varepsilon(Q,\omega)-1$.

[27]J. H. Weaver *et al.*, *Optical Properties of Metals* (Fachinformationszentrum, Karlsruhe, 1981).

[28]U. Kreibig and L. Genzel, Surf. Sci. **156**, 639 (1985).

[29]A. Howie and C. A. Walsh (private communication).

[30]J. D. Jackson, *Classical Electrodynamics,* 2nd ed. (Wiley, New York, 1965).

[31]L. I. Schiff, *Quantum Mechanics,* 2nd ed. (McGraw-Hill, New York, 1955).

[32]G. N. Watson, *Theory of Bessel Functions,* 2nd ed. (Macmillan, New York, 1948), p. 152.

[33]D. Pines, *Elementary Excitations in Solids* (Benjamin, New York, 1964).